AD-A224 728

DTIC FILE COPY

REPORT DOCUMENTATION PAGE

Form Approved
OMB No. 0704-0188

1. AGENCY USE ONLY (Leave blank)	2. REPORT DATE	3. REPORT TYPE AND DATES COVERED
		Final Report/1 Jun 87-31 May 90

4. TITLE AND SUBTITLE
Collisionally Excited XUV and VUV Coherent Sources

5. FUNDING NUMBERS
61102F/2301/A1

(2)

6. AUTHOR(S)
P. Jeffrey Wisoff

7. PERFORMING ORGANIZATION NAME(S) AND ADDRESS(ES)
Rice University
Department of Electrical & Computer Engineering
Houston, TX 77251

8. PERFORMING ORGANIZATION REPORT NUMBER
AFOSR-TR- 90 0809

9. SPONSORING/MONITORING AGENCY NAME(S) AND ADDRESS(ES)
AFOSR/NP
Bolling AFB DC 20332-6448

DTIC ELECTE JUL 26 1990 S D D

10. SPONSORING/MONITORING AGENCY REPORT NUMBER
AFOSR-87-0247

11. SUPPLEMENTARY NOTES

12a. DISTRIBUTION/AVAILABILITY STATEMENT
Approved for public release; distribution is unlimited.

12b. DISTRIBUTION CODE

13. ABSTRACT (Maximum 200 words)

Three types of excitation have been explored including soft x-ray pumping from laser-produced plasmas, electron beam pumping, and pulsed jet discharge pumping. Using the laser produced plasmas, new quasimetastable states of barium which radiate in the XUV have been explored and new VUV radiating molecules have been produced. Electron beam pumping has also resulted in the formation of ionic excimer molecules which radiate in the VUV, and considerable kinetic studies were performed to examine the feasibility of producing a VUV laser by this technique. This included the development of the necessary technology to allow electron beam pumping of reactive vapors at approximately 700 degree C and still maintaining compatibility with VUV detection equipment. Using the third excitation technique, pulsed jet discharge pumping, the formation of highly excited ions from the sputtering of low vapor pressure materials used in the pulsed jet nozzle were studied.

14. SUBJECT TERMS	15. NUMBER OF PAGES
XUV and VUV coherent sources, soft x-ray pumping, electron beam pumping, pulsed jet discharge pumping	25
	16. PRICE CODE

17. SECURITY CLASSIFICATION OF REPORT	18. SECURITY CLASSIFICATION OF THIS PAGE	19. SECURITY CLASSIFICATION OF ABSTRACT	20. LIMITATION OF ABSTRACT
UNCLASSIFIED	UNCLASSIFIED	UNCLASSIFIED	UL SAR

FINAL REPORT FOR

Air Force Office of Scientific Research

Contract #AFOSR-87-0247

Collisionally Excited XUV and VUV Coherent Sources

P. Jeffrey Wisoff

Department of Electrical & Computer Engineering

Rice University

P.O. Box 1892

Houston, Texas 77251

(713) 527-8101, ext. 3567

Table of Contents

I. Summary

During the past three years, the research has focused on excitation techniques and kinetic schemes for producing new XUV and VUV coherent sources. Three types of excitation have been explored including soft x-ray pumping from laser-produced plasmas, electron beam pumping, and pulsed jet discharge pumping. Using the laser produced plasmas, new quasimetastable states of barium which radiate in the XUV have been explored and new VUV radiating molecules have been produced. Electron beam pumping has also resulted in the formation of ionic excimer molecules which radiate in the VUV, and considerable kinetic studies were performed to examine the feasibility of producing a VUV laser by this technique. This included the development of the necessary technology to allow electron beam pumping of reactive vapors at ~700° C and still maintaining compatibility with VUV detection equipment. Using the third excitation technique, pulsed jet discharge pumping, the formation of highly excited ions from the sputtering of low vapor pressure materials used in the pulsed jet nozzle were studied.

A more detailed description of these studies is given in the following sections, as well as in the publications listed in Section IV. Some of these excitation techniques will be studied further under the newly awarded contract AFOSR-90-0257.

II. Description of Project Accomplishments

A. Laser-Produced Plasma Excitation of Barium Ions

Recently, it was shown that the soft x-rays emitted by a laser-produced plasma could be used to excite or photoionize inner shell electrons in atoms [1]. This work led to the discovery of a class of core-excited states in alkali-like atoms and ions which exhibited large radiative yields and relatively slow autoionization rates. As a result of these slow autoionization rates, these states were termed quasimetastable [2]. Due to the radiative character of these states, they appear to be attractive VUV laser candidates, provided large enough densities of such states can be produced. Previous work on these states has concentrated on the excitation of quasimetastable states in alkalis using hot photoelectrons generated by the soft x-rays from a laser-produced plasma to collisionally excite core electrons in the alkali metal atoms.

At Rice University VUV emission from Ba^+ ions, which may be due to such quasimetastable levels, has been investigated. The advantage of studying emission from the ions of Column II elements is that by proper laser preparation of the neutral vapor states, efficient photoionization into the desired quasimetastable level can be achieved rather than relying on electronic collisional excitation.

To explore this possibility, barium was chosen as a likely candidate. Soviet researchers had previously observed intense emission at 71.2 nm from an unidentified core-excited level of Ba^+ using crossed electron and atomic beams [3]. Recently, we have observed this line in *Ba* vapor confined in a heatpipe cell using the soft x-rays from a ~10 ns long, Nd:YAG laser-produced plasma as an excitation source. Another unidentified VUV line at 68.5 nm was also apparent in our initial experiments [4].

In order to understand the source of these emissions, dye laser transfer experiments have been performed. The goal of these experiments was to study the relative emission at 71.2 nm and 68.5 nm when ground state Ba atoms were photoionized, in comparison to the photoionization of Ba atoms that are first prepared in the $(5p^6\,6s\,5d)^3D$ metastable levels. As shown in Fig. 1, population is moved from the $Ba(5p^6\,6s^2)\,^1S_o$ ground state to the $Ba(5p^6\,6s\,5d)^3D$ levels. This is accomplished by tuning a dye laser to 791 nm which corresponds to the $Ba(5p^6\,6s^2)\,^1S_o \rightarrow Ba(5p^6\,6s\,6p)^3P$ transition. The population decays from the ^3P levels into the $Ba(5p^6\,6s\,5d)^3D$ levels which are metastable. Once these metastable levels are filled, the $Nd:YAG$ laser is focused onto a tantalum target inside the Ba heat-pipe cell, producing a plasma which radiates soft x-rays. These soft x-rays efficiently remove inner shell electrons producing core-excited Ba^+ states. Inner shell electrons are preferentially removed due to the high degree of overlap between the wavelength dependence of the inner shell photoionization cross sections and the soft x-ray emission spectrum from the laser-produced plasma.

The results of these dye laser transfer experiments are consistent with the hypothesis that the 68.5 nm emission originates from the $Ba^+(5p^5\,6s\,5d)\,^4F_{3/2}$ state and that the 71.2 nm line originates from the $Ba^+(5p^5\,5d^2)\,^4F_{3/2}$ level. As indicated in Fig. 1, only the 68.5 nm emission was enhanced by the dye laser transfer. Since this transfer process would favor the formation of the $5p^5\,6s\,5d$ configuration by the photoionization of a single p electron from the metastable $Ba(5p^6\,6s\,5d)^3D$ levels, the 68.5 nm probably originates from such a configuration. Both of the preliminary assignments correspond to levels satisfying the quasi-metastable criteria described in Reference [2] and, therefore, would be expected to exhibit high radiative yields in the VUV. Furthermore, our preliminary identifications are consistent with the predicted wavelengths from a Dirac-Fock calculation in Reference [5]:

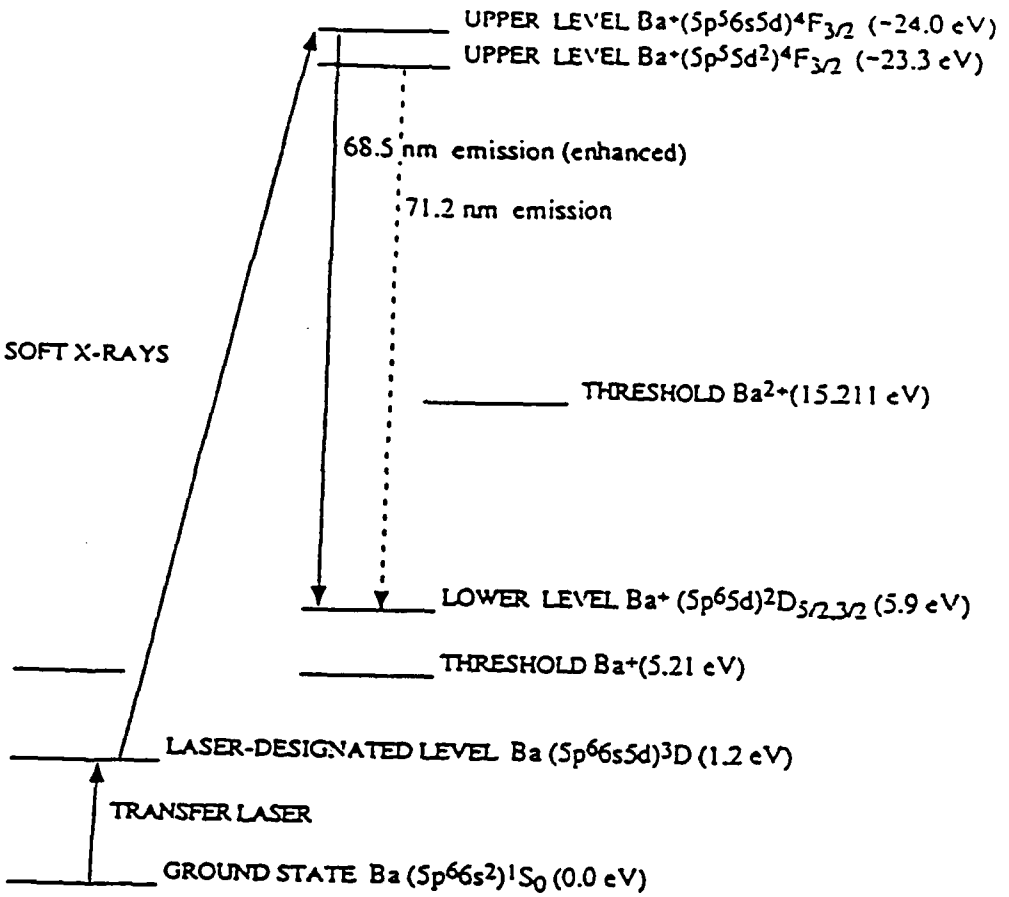

Figure 1: Schematic of Ba^+ system. Population is transferred to the metastable ^3D levels of neutral *Ba* and then photoionized using the soft x-rays from a laser-produced plasma. The emission on the 68.5 nm line is enhanced relative to the observed emission when ground state *Ba* atoms are photoionized. The 71.2 nm emission is unaffected by the transfer to the ^3D levels. Preliminary upper state assignments for the VUV emission are shown.

Proposed transition	*Ref.* [5] *calculation*	*Experiments*
$Ba^+(5p^5\,6s\,5d)^4F_{3/2} \rightarrow Ba^+(5p^6\,5d)^2D_{3/2,}$	67.5 nm	68.5 nm
$Ba^+(5p^5\,5d^2)^4F_{3/2} \rightarrow Ba^+(5p^6\,5d)^2D_{3/2,}$	72.2 nm	71.2 nm

Although these identifications are preliminary, these experiments provide a first step in unraveling thc very complex core-excited manifold of Ba^+. In addition, the ability to enhance VUV emission from core-excited states using preparation of the initial state before pumping by a

laser-produced plasma demonstrates that the potential number of viable VUV laser transitions can be increased by this technique.

To achieve gain in such systems, it is important to use a fast excitation source in order to create an inversion and to minimize population loss through autoionization. This need to minimize autoionization losses has recently been demonstrated by the realization of a *Cs* laser at 97 nm by electronic excitation of neutral *Cs* to a core-excited state [6]. In order to observe significant radiative yield from this core-excited state, the stimulated emission rate must be faster than the autoionization rate. To achieve this, picosecond laser-produced plasma pumping was used. The need for such ultrafast laser plasmas indicates that technologies must be developed which can produce very high intensity ultrashort pulses if this method is to be extended to x-ray laser systems which often have higher decay rates. To address these needs, research at Rice University is continuing on the development of new ultrashort laser pulse amplifiers.

B. Production of VUV Radiating Molecules by Laser Plasma Excitation

Previous investigations with laser-produced plasmas have focused on photoionizing or exciting atomic species to produce VUV radiation. Recently, however, in collaboration with Prof. R. Sauerbrey at Rice University, we have demonstrated that reactive kinetics can be driven by a laser-produced plasma to produce radiating molecules [7]. Specifically, laser-produced plasma excitation has been used to produce fluorescence from the well-known *XeF* excimer at 351 nm and from a new ionic excimer $(XeRb)^+$ at 165 nm.

The apparatus used in this work is shown in Fig. 2 [7]. The output of an oscillator-amplifier injection-controlled *KrF* laser was focused onto a *Ta* target inside a stainless-steel oven. The soft x-rays emitted from the laser-produced plasma photoionize the surrounding gas

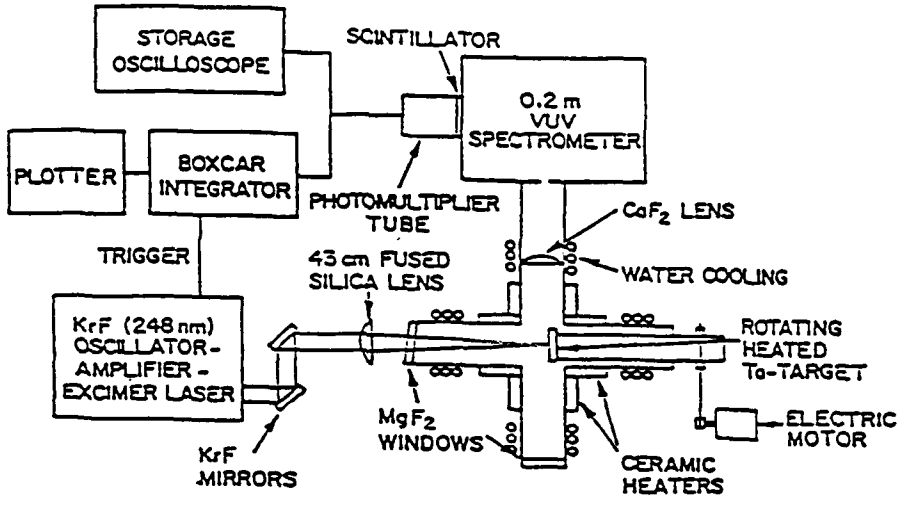

Figure 2: Experimental setup. A focused *KrF* excimer laser generates a plasma on a *Ta* target inside a heated cell. The soft x-rays emitted from the plasma photoionized the surrounding vapor, leading to the formation of excimer or ionic excimer species.

or vapor, leading to the formation of molecules. The oven, capable of producing *Rb* vapor with a pressure as high as 10 Torr, was configured as a crossed-arm cell that permitted viewing of the target region perpendicular to the direction of the focused *KrF* laser beam. The *Ta* target was heated to prevent condensation of *Rb* upon the surface and was rotated to provide a new surface for successive laser shots. The *KrF* laser provided a 750 mJ pulse with a duration of 30 nsec in a 1.5 cm × 3 cm rectangular mode at a repetition rate of 2 Hz. When a lens with a focal length of 22.5 cm at 248 nm was used, the intensity on the target was approximately 5×10^{10} W/cm^2.

A 10 cm focal-length CaF_2 or MgF_2 lens was used to collect the fluorescence from the interaction zone and to focus it onto the entrance slit of a 0.2 m VUV spectrometer. The *Ta* target was located approximately 0.5 cm from the optical axis of the spectrometer. A photomultiplier tube equipped with a sodium salicylate scintillator provided time-resolved fluorescence data in conjunction with a high-speed storage scope. The measured rise time of this

detection system was approximately 5 nsec. Time-averaged spectra were obtained by using a boxcar integrator with a 50 nsec gate to discriminate against recombination radiation from the *Ta* plasma, which appeared approximately 200 nsec after the laser pulse [7].

The fluorescence of $(XeRb)^+$ as a function of *Rb* pressure which was measured using this apparatus is shown in Fig. 3. This is the first reported observation of molecular formation from constituent atomic species as a result of laser-plasma pumping.

The significance of this result is that new approaches to the production of VUV and XUV lasers utilizing reactive kinetics in laser-produced plasmas can now be explored. Such approaches include new excimer lasers [8,9] and photodissociation of molecules into desired

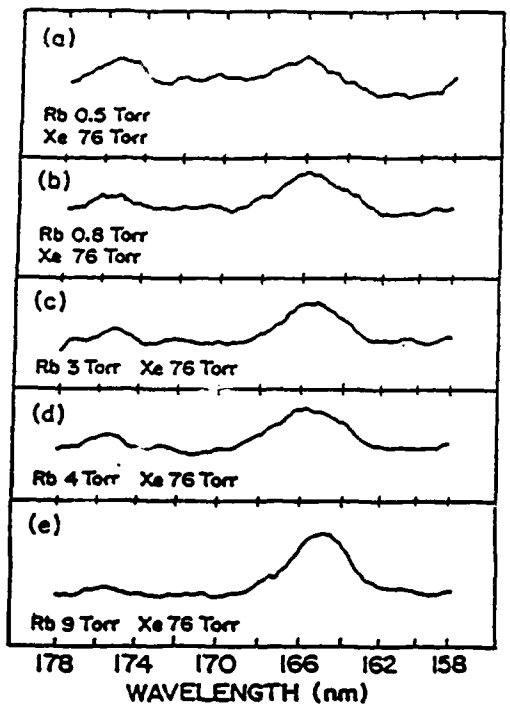

Figure 3: Time-integrated fluorescence from $(XeRb)^+$ for different pressures of *Rb* at 76 Torr of *Xe*.

target species followed by soft x-ray excitation. The second of these approaches may be desirable if the target state can be produced by molecular photodissociation, as opposed to utilizing an atomic vapor which may be absorbing at the desired radiation wavelength or difficult to produce due to temperature limitations.

C. Electron Beam Excitation of Rare Gas-Alkali Ionic Molecules

In order to further explore the feasibility of producing lasers with new ionic molecules such as $(XeRb)^+$, electron beam excitation was investigated as a possible pumping mechanism. Electron beam pumping offers the advantage of operating at high pressures allowing significant molecular formation, and in addition, this type of excitation provides long active lengths of 10 cm or more.

In order to use this technique of pumping, however, a heated alkali-compatible electron beam cell had to be developed [10]. Other excitation techniques such as laser-produced plasmas and electrical discharges have relied largely on conventional heatpipe technology which produces a well-defined vapor column at typically a few Torr of pressure; however, electron beam excitation, using MeV electrons, requires high pressure buffer gases to effectively absorb the delivered energy in a small volume. The experimental apparatus cannot rely, therefore, on heatpipe technology since, generally, a high pressure of a noble gas such as *Ar* must be added to the few Torr of the active medium in order to absorb the electron beam energy. Previous heated electron beam cells have been designed for operation with dye vapors and metals for visible or near UV wavelengths and have been limited to temperatures of 600° C or less [11,12]. The cell design developed for this research, shown in Fig. 4, can operate up to 750° C with over 700 shots before changing foils. To further enhance the deposited pump energy density in the cell, a large magnet has been constructed to surround the electron beam apparatus. This magnet

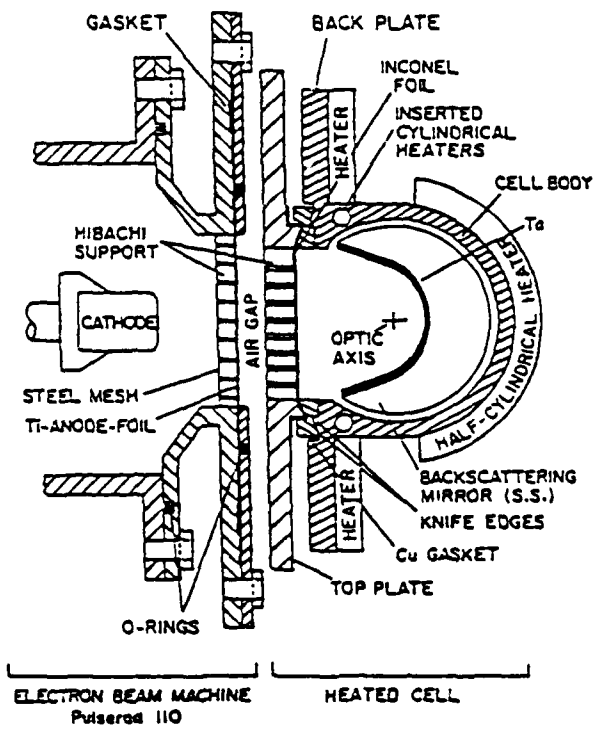

Figure 4: Cross-sectional view of heated cell and electron beam cathode. Heated cell is sealed with Iconel foil, and the cathode region is sealed with titanium foil. The small air gap acts as a thermal insulator.

produces a quasi-D.C. magnetic field of approximately 3 kilo-Gauss to prevent spreading of the electron beam. Fig. 5 shows the newly developed cell attached to the VUV diagnostics used during the experiments. Windowless VUV techniques have also been developed over the course of this research to study the radiation of species which emit below the cut-off of *LiF* windows.

Using this experimental set-up, in collaboration with Prof. R. Sauerbrey, we have successfully demonstrated electron beam excitation of both $(XeRb)^+$ and $(XeCs)^+$ [13]. $(XeRb)^+$ is found to radiate at 164 nm and $(XeCs)^+$ radiates at 160 nm. The fluorescence spectrum for $(XeRb)^+$ is shown in Fig. 6. Preliminary identification of the electronic transitions correspond-

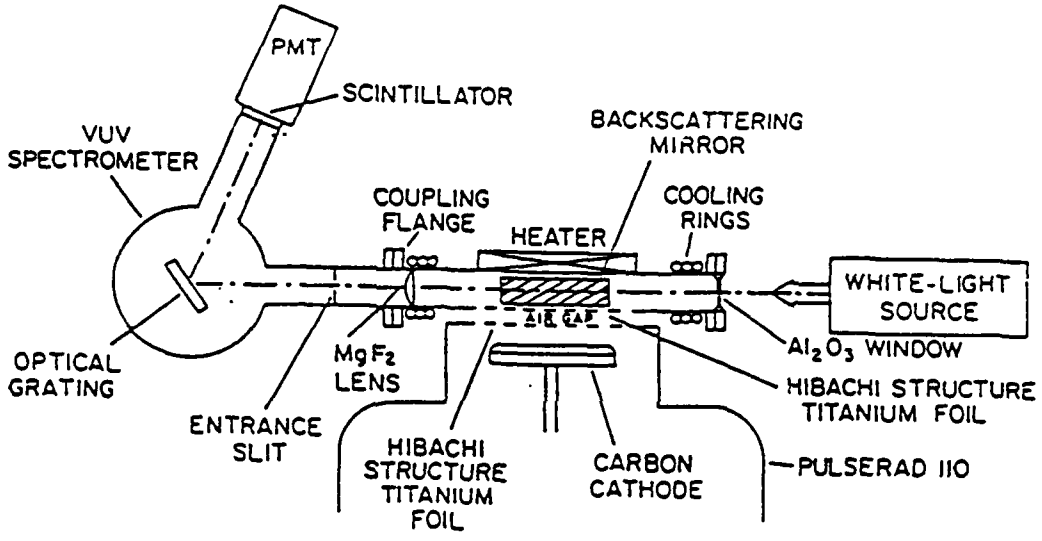

Figure 5: Top view of heated cell, VUV detection apparatus, and electron beam machine. The dye laser or white-light source can be used to measure population densities in the hot vapor.

ing to the three peaks of Fig. 6 have also been assigned [13]. Fig. 7 shows the simple exponential behavior of the fluorescence decay of $(XeCs)^+$. By fitting the temporal behavior of the fluorescence emission from $(XeCs)^+$ and $(XeRb)^+$, preliminary values of the dominant kinetic coefficients have been determined [7]. Since the emission from the $(XeCs)^+$ molecule is comparable to that of Xe_2^*, we feel that this species is a very viable laser candidate. Work is continuing on this system.

D. Pulsed Jet Discharge Excitation

Recently, a high voltage, high current discharge through a pulsed supersonically expanding gas has been reported as a potential VUV laser excitation mechanism [14]. These discharges are designed with an electrode immediately behind the orifice of a pulsed jet with a grounded wire mesh located about 1.5 cm below the nozzle orifice. This arrangement achieves high peak currents and a very high current density since the discharge is confined to the small area of the nozzle orifice. This approach differs from other recent work [15-20] in that the discharge

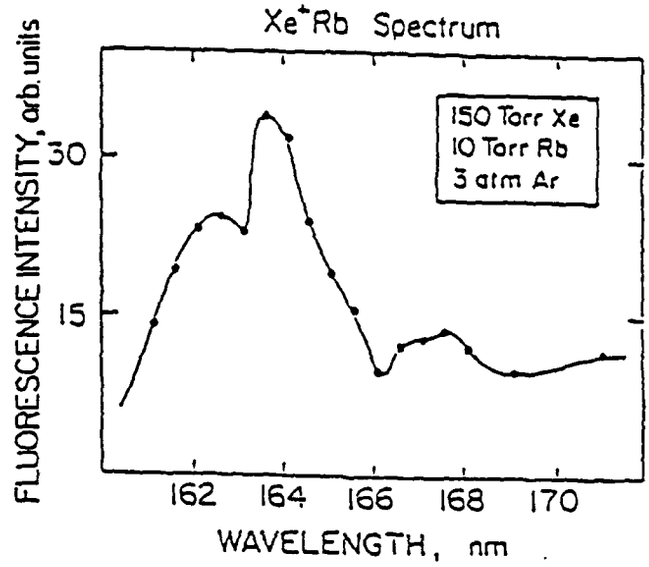

Figure 6: $(XeRb)^+$ fluorescence spectrum resulting from an electron beam excited mixture of *Ar/Xe/Rb*. The resolution is 0.8 nm. Each date point corresponds to an individual electron beam shot. The solid line is for presentation purposes.

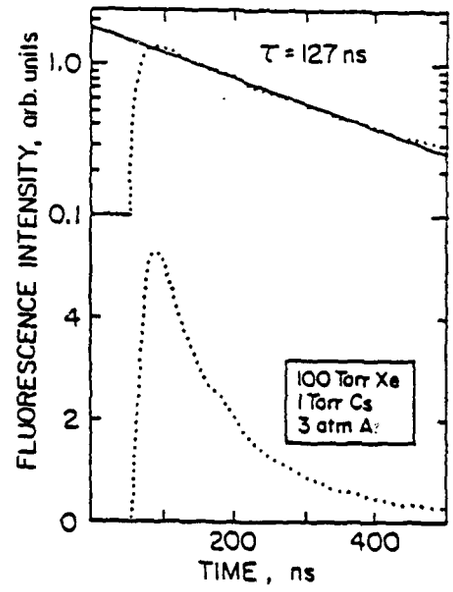

Figure 7: Temporal behavior of the VUV fluorescence of $(XeCs)^+$ at 160 nm. The upper plot of the emission displays the logarithm of the observed temporal profile. The line fitted through this plot results from a single exponential decay with an effective decay time τ.

duration is short (~100 ns), and currents in excess of 1 KA are employed.

Although the initial design and operation of these discharges with Ar was outlined in Ref. 14, the characterization of this device with respect to nozzle design, gas parameters, and discharge current was incomplete. At Rice University the visible ultraviolet and vacuum ultraviolet (VUV) emission spectra resulting from the gas in the pulsed nozzle as well as from the sputtered material from the nozzle itself have been investigated [21].

A schematic of the pulsed jet discharge system is shown in Figure 8. A pulsed valve (General Valve) is located on top of the nozzle assembly and sends a short (≈1 ms) pulse of gas through the orifice of the nozzle into the vacuum chamber. While the gas expands through the nozzle, a discharge through the nozzle towards the grounded grid is initiated. The back pressure on the valve was maintained at about 3 atm. The gases studied included He, N_2, Ne, Ar, Kr, Xe, NF_3, and SF_6. A turbo pump backed by a rotary vane roughing pump restored the

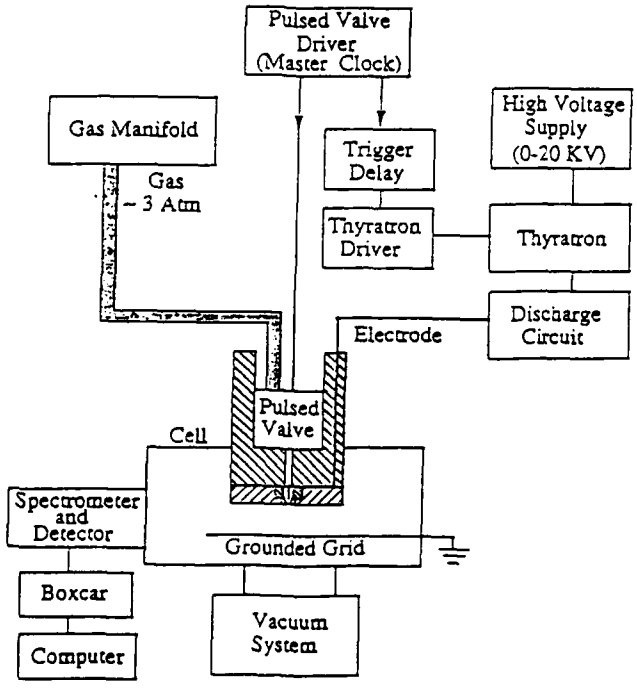

Figure 8: Schematic of the pulsed jet discharge and the VUV detection apparatus.

background pressure in the cell to a few times 10^{-5} Torr between pulses when the discharge was operated at low repetition rates (1-2 Hz). The tungsten electrode was situated about 1.5 mm above the nozzle orifice, and a stainless steel wire mesh located 1.5 cm below the orifice served as the ground plane. Details of the apparatus and the discharge circuit are given in Ref. 21 (preprint attached).

The nozzle assembly was designed so that the nozzle was interchangeable, and a variety of orifice diameters and nozzle materials could be studied. The nozzle orifices ranged from 250 to 500 μm in diameter. Materials used for the nozzles included Macor, a machinable ceramic, sapphire, glass, carbon, Delrin, and PVC. The nozzles were designed to give a supersonic expansion and to optimize the production and cooling of molecular radicals and ions [18]. All of the nozzles made from machinable materials and the sapphire nozzles had a 45° half angle above the nozzle orifice on the high pressure side, and a 90° half angle on the vacuum side. The glass nozzles were made from glass tubing which was heated and tapered at approximately a 45° half angle until the orifice was about 500 μ. Photographs of the discharge indicated the presence of a Mach disk about 1 cm below the nozzle.

Spectroscopic studies were performed with a scanning 0.2 m VUV spectrometer (Acton Research Corp.) using a photomultiplier with a scintillator as the detector with a temporal resolution of ~10 ns. The spectral resolution of the system was approximately 5 Å . The optical axis of the spectrometer was aligned to be approximately 2 mm below the nozzle orifice, corresponding to the point of brightest VUV fluorescence. This was determined experimentally by measuring the fluorescence intensity of several bright VUV lines as a function of the distance from the nozzle, with 1 mm resolution using a movable slit. The signal was averaged with a boxcar integrator, and the data were stored and processed in a computer. Temporal

waveforms were obtained with a 400 MHz bandwidth oscilloscope.

The emission spectra from the pulsed jet discharge were studied in the wavelength range between 35 nm and 550 nm using different gas species in the pulsed jet and a variety of nozzle materials. All of the spectra presented here have not been corrected for the spectral response of the detection system. With lighter gases such as *He*, spectra dominated by the gas species were obtained. An example of a spectrum obtained with *He* and a nozzle made of Macor is shown in Figure 9. All of the bright emission lines can be assigned to excited helium atoms and ions. To obtain these spectra, the gate on the boxcar was set to a width of 75 ns and was delayed 250 ns after the peak of the current pulse. This time window for observation was chosen because the spectra measured at various time delays indicated that many spectral lines were more prominent during this time window. All bright emission lines can be assigned to excited helium atoms and ions.

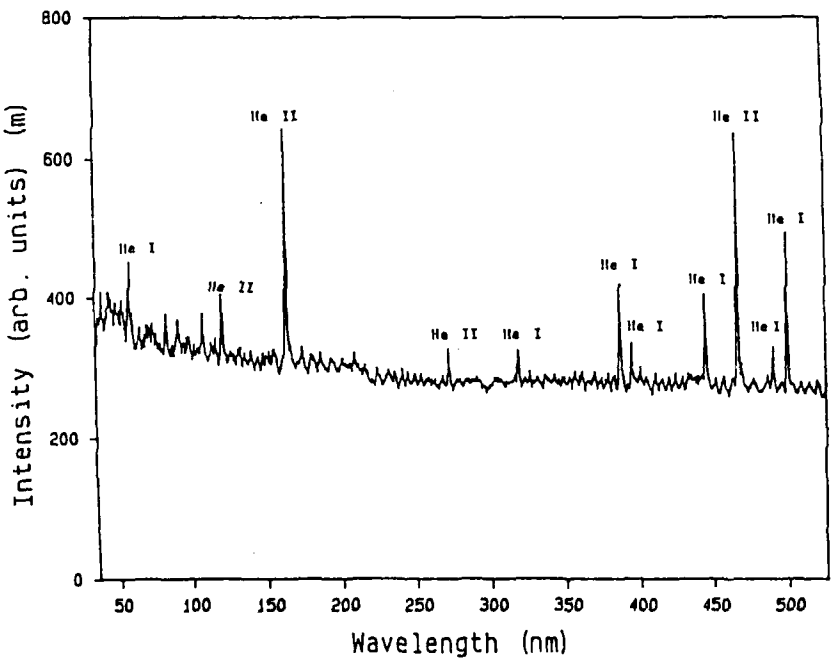

Figure 9: Emission spectrum at 15 KV charging voltage, taken 250 ns after the peak of the current pulse, with *He* as the gas species and using a Macor nozzle.

With *Ar* and other heavier gases, however, the spectra obtained were quite different. While the visible spectrum obtained with *Ar* is dominated by lines from *Ar II* and *Ar III*, the VUV spectrum is dominated by lines from the sputtered nozzle material. Figure 10 shows the VUV spectrum obtained using *Ar* with a sapphire nozzle. The time window for observation was identical to that used for the *He* spectrum. The dominant features are aluminum and oxygen lines originating from the sputtering of the sapphire (Al_2O_3) nozzle. Sputtering is due to the effective momentum transfer from the gas ions to the nozzle material. Typical ion kinetic energies inside the nozzle can be estimated to be 10 eV to several hundred eV. In this energy range efficient sputtering of the nozzle material by heavier rare gases is expected, whereas the sputtering efficiency of *He* is low [22].

When Macor is used as the nozzle material, the VUV spectra with the heavier gases are dominated with *Si* and *Al* lines. An example with *Ar* as the gas species is shown in

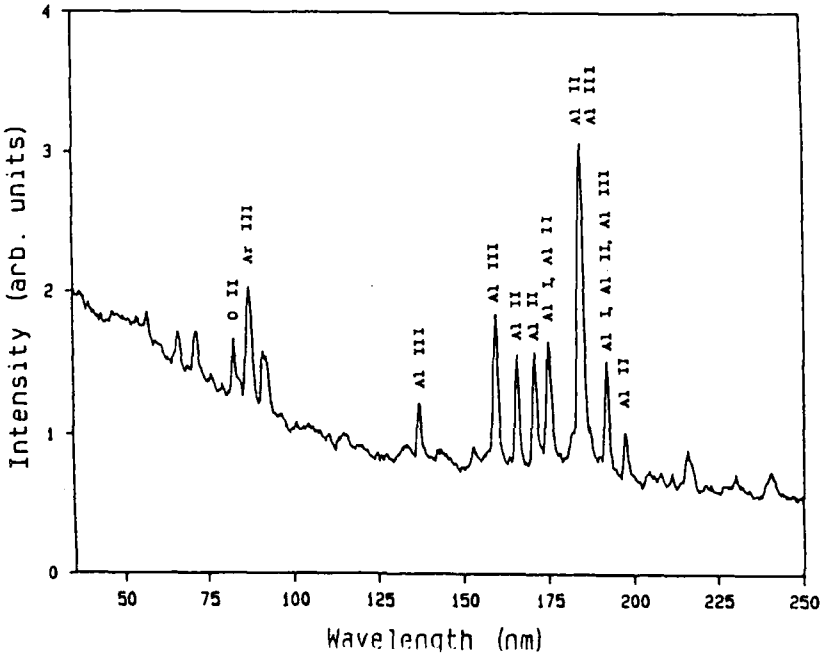

Figure 10: Emission spectrum at 17.5 KV charging voltage, taken 250 ns after the peak of the current pulse, with *Ar* as the gas species and using a sapphire nozzle.

Figure 11. Macor has a complicated chemical composition, but some of the major constituents are SiO_2 (46%) and Al_2O_3 (16%). Spectra obtained with glass nozzles show many of the same Si lines. Spectra taken with carbon, PVC, or Delrin nozzles exhibit strong carbon lines.

The high degree of excitation and ionization is a result of the initial confinement of the discharge to the small orifice allowing very high current densities (~ 1 MA/cm^2) to be achieved. Some of the spectral lines which have been identified as arising from the sputtering of the nozzle material indicate the formation of states as much as 45 eV above the ground state of the neutral species. Such pulsed jet discharges could therefore have applications in spectroscopic studies of highly excited states of materials that are difficult to evaporate, or in the development of incoherent VUV light sources for other spectroscopic investigations.

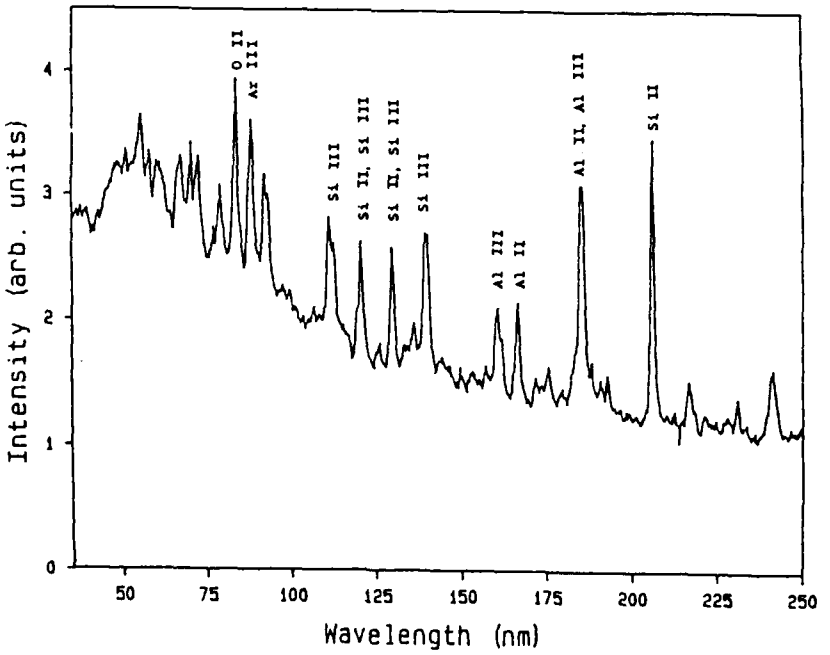

Figure 11: Emission spectrum at 15 KV charging voltage, taken 250 ns after the peak of the current pulse, with Ar as the gas species and using a Macor nozzle.

In Ref. 14, emission from the excimer Ar_2^* around 126 nm was reported using a pulsed jet discharge with similar discharge parameters. In the work reported here, the region around 126 nm was extensively studied with various nozzles and at various discharge voltages, but no evidence of emission from Ar_2^* was detected. Searches for other excimer emissions – such as He_2^*, Kr_2^*, ArF, KrF, and XeF – were also performed, but no emission from these species in such a high current pulsed jet discharge was observed.

III. References:

[1] R.G. Caro, J.C. Wang, R.W. Falcone, J.F. Young, and S.E. Harris, "Soft X-ray Pumping of Metastable Levels of Li^+," *Appl. Phys. Lett.* 42, 9-11 (1983).

[2] S.E. Harris, D.J. Walker, R.G. Caro, A.J. Mendelsohn, and R.D. Cowan, "Quasi-Metastable Quartet Levels Alkali-Like Atoms and Ions," *Opt Lett.* 9, 168-170 (1984).

[3] I.S. Aleksakhin, G.G. Bogachev, and S. Yu Ugrin, "Investigation of the *Ba* Emission Spectra in the 50-90 nm Region with Electron Impact Excitation of Atoms," *Opt. Spectros.* 43, 476 (1977).

[4] T. Petersen, Rice University Master's Thesis (Apr. 1989).

[5] S.J. Rose, I.P. Grant, and J.P. Connerade, "A Study of 5*p* Excitation in Atomic Barium II. A Fully Relativistic Analysis of 5*p* Excitation in Atomic Barium," *Phil. Trans. Royal Society of London,* 296, 527 (1980).

[6] C.P.J. Barty, D.A. King, G.Y. Yin, K.H. Hahn, J.E. Field, J.F. Young, and S.E. Harris, "12.8 eV Laser in Neutral Cesium," *Phys. Rev. Lett.* 61, 2210 (1988).

[7] P. Millar, T. Petersen, G. Warwar, P.J. Wisoff, and R. Sauerbrey, "Neutral and Ionic Excimer Molecules Produced by Reactive Kinetics in a Laser-Produced Plasma," *Opt. Lett.* 14, 171 (1989).

[8] R. Sauerbrey and H. Langhoff, "Excimer Ions as Possible Candidates for VUV and XUV Lasers," *IEEE J. Quant. Electr.* QE-21 (3), 179 (1985).

[9] N.G. Basov, M.G. Voĭtik, V.S. Zuev, and V.P. Kutakhov, *Soviet J. of Quant. Electr.* 15, 1455 (1985).

[10] T. Petersen, P.S. Millar, L. Frey, F.K. Tittel, W.L. Wilson, Jr., R. Sauerbrey, and P.J.K. Wisoff, "A Heated Cell for Electron Beam Pumped VUV Experiments," *Rev. of Scient. Instr.* 59 (12), 2596 (1988).

[11] G. Marowsky, R. Cordray, F.K. Tittel, and W.L. Wilson, *Appl. Opt.* 17, 3491 (1978).

[12] F.B Haller, M.M. Hessel, W. Neef, W. Lai, and H. Lohr, Symposium on Engineering Problems of Fusion Research, 6th Proceedings, San Diego, CA (Nov. 18-23, 1978), 79-83.

[13] P.S. Millar, G. Warwar, P.J. Wisoff, R. Sauerbrey, and K. Balasubramanian, "Electron Beam Excitation of Rare-Gas Alkali Ionic Excimers," *Appl. Phys. Let.* 55, 2176 (1989)

[14] T. Epthimiopoulos, B.P. Stoicheff, and R.I. Thompson, "Efficient Population Inversion in Excimer States by Supersonic Expansion of Discharge Plasmas," *Opt. Lett.* 14, 624-626 (1989).

[15] C. Jouvet, C. Lardeaux-Dedonder, and D. Solgadi, "Fluorescence Excitation Spectra of the *XeCl(B,C)* States in a Supersonic Jet," *Chem. Phys. Let.* 156 (6), 569-572 (21 April 1989).

[16] C.S. Feigerie and J.C. Miller, "Multiphoton Ionization of Vibrationally Hot Nitric Oxide Produced in a Pulsed Supersonic Glow Discharge," *J. Chem. Phys.* 90 (6), 2900-2908 (15 March 1989).

[17] K.G.H. Baldwin, R.P. Swift, and R.O. Watts, "Inert Gas Excimer Radiation from a Free Jet Expansion," *Rev. Sci. Instrum.* 58 (5), 812-816 (May 1987).

[18] P.C. Engelking, "Corona Excited Supersonic Expansion," *Rev. Sci. Instrum.* 57 (9), 2274-2277 (September 1986).

[19] K.P. Huber and T.J. Sears, "Emission Spectra in a Supersonic Expansion: The Quartet System of *NO* and the Schüler Band of ND_4," *Chem. Phys. Let.* 113 (2), 129-134 (11 January 1985).

[20] A.T. Droege and P.C. Engelking, "Supersonic Expansion Cooling of Electronically Excited Radicals," *Chem. Phys. Let.* 96 (3), 316-318 (8 April 1983).

[21] A.B. Glaser and G.E. Subak-Sharpe, *Integrated Circuit Engineering,* Reading, MA: Addison-Wesley, 1977, pp. 169-181.

[22] H. Phillips, S. Kubodera, R. Sauerbrey, F.K. Tittel, and P.J. Wisoff, "Characterization of Plasmas from a Pulsed Jet Discharge for Applications to VUV Spectroscopy and to Micromechanics," to be published.

IV. Publications and Conference Reports

1. "A Heated Cell for Electron Beam Pumped VUV Experiments," *Rev. Scient. Instr.* 59 (1988), pp. 2596-2599, with P. Millar, T. Petersen, L. Frey, W.L. Wilson, Jr., F.K. Tittel, and R. Sauerbrey.

2. "Core-Excited Alkali Atoms and Ionic Excimers as VUV/XUV Laser Sources," *Proceedings of International Conference on Lasers '87* (1988), p. 160, with L. Frey, S. Kubodera, P.S. Millar, T. Petersen, G. Warwar, and R. Sauerbrey.

3. "Neutral and Ionic Excimer Molecules Produced by Reactive Kinetics in a Laser-Produced Plasma," *Optics Letters* 14 (1989), p. 171-173, with P. Millar, T. Petersen, G. Warwar, and R. Sauerbrey.

4. "Ionic Excimers," *Proceedings of the International Conference on Lasers '88*, Lake Tahoe, NV, Dec. 4-9, 1988, Invited Paper FA.1, with S. Kubodera, P.S. Millar, G. Warwar, and R. Sauerbrey.

5. "Ionic Excimers Excited by Laser-Produced Plasmas," *Technical Digest of the XVI International Conference on Quantum Electronics* (IQEC) (July 1988), pp. 224-225, with R. Sauerbrey, S. Kubodera, and L. Frey.

6. "Progress Toward Rare Gas-Alkali Metal Ionic Molecular Lasers," Conference on Quantum Electronics and Laser Science (QELS '89), Baltimore, MD (April 24-28, 1989), with P. Millar, G. Warwar, and R. Sauerbrey.

7. "Electron Beam Excitation of Rare-Gas Alkali Ionic Excimers," *Appl. Phys. Lett. 55, 2176, with P.S. Millar, G. Warwar, and R. Sauerbrey.*

8. "Ionic Excimers Generated by Electron Beams and Laser Produced Plasmas," Engineering Foundation Conference on Future Prospects and Applications for UV and VUV Lasers II, Santa Barbara, CA, Feb. 25-March 2, 1990, with S. Kubodera, P.S. Millar, and R. Sauerbrey.

9. "Characterization of Plasmas from a Pulsed Jet Discharge," Conference on Lasers and Electro-Optics (CLEO '90), Anaheim, CA, May 21-25, 1990, with H. Phillips, S. Kubodera, R. Sauerbrey, and F.K. Tittel.

10. "Characterization of Plasmas from a Pulsed Jet Discharge for Applications to VUV Spectroscopy and to Micromechanics," submitted to *IEEE Journal of Quantum Electronics*, with H. Phillips, S. Kubodera, R. Sauerbrey, and F.K. Tittel.

Characterization of Plasmas from a Pulsed Jet Discharge for Applications to VUV Spectroscopy and to Micromechanics

H. Phillips, S. Kubodera, R. Sauerbrey, F.K. Tittel, and P.J. Wisoff

Department of Electrical and Computer Engineering and

Rice Quantum Institute

Rice University

P.O. Box 1892

Houston, Texas 77251

Abstract

Plasmas from a pulsed jet discharge have been characterized with respect to gas species and nozzle design. Spectral lines from the gas used in the pulsed nozzle are apparent in the visible region. The vacuum ultraviolet spectrum, in particular for heavier gases, is dominated by emission from species sputtered from the nozzle. The production of highly ionized and excited states from materials created by the sputtering of the nozzle has possible applications in VUV spectroscopy. By operating the pulsed jet discharge at a 50 Hz repetition rate with NF_3 to produce excited fluorine ions, etch rates in excess of 10 μm/min have been achieved in silicon which may have applications to micromechanics.

I. Introduction

Recently, a high voltage, high current discharge through a pulsed, supersonically expanding gas has been reported as a potential VUV laser excitation mechanism [1]. These discharges are designed with an electrode immediately behind the orifice of a pulsed jet with a grounded wire mesh located about 1.5 cm below the nozzle orifice. Such an arrangement achieves high peak currents (~2 KA) and a very high current density (~ 1 MA/cm^2) since the discharge is confined to the small area of the nozzle orifice. This approach differs from other recent work [2-7] in that the discharge duration is short (~100 ns), and currents in excess of 1 KA are employed.

Although the initial design and operation of these discharges with *Ar* was outlined in Ref. 1, the characterization of such a device with respect to nozzle design, gas parameters, and discharge current needed further study. *In this work the visible, ultraviolet, and vacuum ultra-*violet (VUV) emission spectra resulting from the excitation of the gas in the pulsed nozzle as well as from the sputtered material from the nozzle itself are investigated.

In addition to these spectroscopic studies, fluorine component gases such as NF_3 have been used in the discharge in order to etch silicon. The results may have applications to micromechanics where high etch rates are necessary to produce relatively large but deep feature sizes (~10-100 μm) in contrast to microelectronics where small feature sizes ($\lesssim 1$ μm) are required at relatively shallow depths.

II. Description of Discharge Apparatus

A schematic of the pulsed jet discharge system is shown in Figure 1. A pulsed valve (General Valve) is located on top of the nozzle assembly and sends a short ($\approx$1 ms) pulse of gas through the orifice of the nozzle into the vacuum chamber. While the gas expands through the nozzle, a discharge through the nozzle towards the grounded grid is initiated. The back pressure on the valve is maintained at about 3 atm. The gases studied included He, N_2, Ne, Ar, Kr, Xe, NF_3, and SF_6. A turbo pump backed by a rotary vane roughing pump restores the background pressure in the cell to a few times 10^{-5} Torr between pulses when the discharge is operated at low repetition rates (1-2 Hz). The tungsten electrode is situated about 1.5 mm above the nozzle orifice, and a stainless steel wire mesh located 1.5 cm below the orifice serves as the ground plane.

The high voltage discharge circuit is shown in Figure 2. The maximum voltage from the power supply is 20 KV. The capacitance of the charging capacitor (C1) is 5.6 nF, and that of the peaking capacitor (C2) is 4.2 nF. With a thyratron (EG&G HY-3202) serving as the high voltage switch, the current pulse, measured by a commercial current transformer, has a FWHM of about 100 ns, with some ringing out to about 1 μs. At 15 KV charging voltage, the peak current is 1.8 KA. For a 500 μm diameter orifice, this peak current corresponds to an average current density of 0.9 MA/cm^2 inside the orifice. The trigger output of the pulsed valve is used as the master clock, but a trigger delay of about 1 ms for the thyratron is required for a stable discharge; i.e., the discharge is initiated about 1 ms after the beginning of the jet expansion.

Figure 3 shows typical voltage and current waveforms. Because of the finite inductance of the electrode, the voltage peaks approximately 80 ns before the current. Assuming the value of the peaking capacitor (4.2 nF) is fixed, the ringing period of the current indicates that the induc-

tance of the discharge is about 290 nF. The decay of the current ringing reveals that the resistance of the discharge reaches a value of approximately 3-4 Ω. Integration of the power calculated using these waveforms gives an estimate of the energy delivered to the discharge of about 200mJ during the initial current pulse. The small bump in the decay of the initial current pulse (at ~250 ns on Fig. 3) is apparently due to a surge of current from the outer circuit loop which includes the storage capacitor and the thyratron.

At higher charging voltages, there seems to be significant energy dissipated during the ringing period of the discharge. From the current and voltage waveforms, it can be seen that there is a secondary peak of energy dissipation approximately 200 ns after the initial peak, with additional peaks occuring with a period of roughly 100 ns. This feature can also be seen in the temporal behavior of the fluorescence. Figure 4 shows traces of the temporal response of the 207 nm emission from *Si II*, which is very bright in spectra taken with a Macor or glass nozzle using heavy gases in the pulsed jet. At a discharge voltage of 15 KV(a), the signal decays after about 100 ns, corresponding to the decay of the initial peak of the discharge current. At 20 KV(b), however, the intensity becomes very broad in time and shows a pronounced periodic structure in its decay. When the transit time of the photomultiplier (~30 ns) is taken into account, the second fluorescence peak is delayed about 200 ns from the initial peak of the discharge, and the period of the later fluorescence peaks at about 80-100 ns, which is in good agreement with the analysis of the voltage and current waveforms.

The nozzle assembly is designed so that the nozzle is interchangeable, and therefore, a variety of orifice diameters and nozzle materials can be studied. Discharge operation with nozzle orifices ranging from 250 to 500 μm in diameter has been characterized. Materials used for the nozzles include Macor, (a machinable ceramic), sapphire, glass, carbon, Delrin, and PVC.

The nozzles are designed to give a supersonic expansion and to optimize the production and cooling of molecular radicals and ions[5]. All of the nozzles made from machinable materials and the sapphire nozzles have a 45° half angle above the nozzle orifice on the high pressure side, and a 90° half angle on the vacuum side. The glass nozzles are made from glass tubing which is heated and tapered at approximately a 45° half angle until the orifice is about 500 μm. Photographs of the discharge indicate the presence of a Mach disk about 1 cm below the nozzle.

Spectroscopic studies were performed with a scanning 0.2 m VUV spectrometer (Acton Research Corp.) using a photomultiplier with a scintillator as the detector with a temporal resolution of ~10 ns. The spectral resolution of the system was approximately 5 Å. The optical axis of the spectrometer was aligned to be approximately 2 mm below the nozzle orifice, corresponding to the point of brightest VUV fluorescence. This was determined experimentally by measuring the fluorescence intensity of several bright VUV lines as a function of the distance from the nozzle, with 1 mm resolution using a movable slit. The signal was averaged with a boxcar integrator, and the data were stored and processed in a computer. Temporal waveforms were obtained with a 400 MHz bandwidth oscilloscope.

III. Spectroscopic Results

The emission spectra from the pulsed jet discharge were studied in the wavelength range between 35 nm and 550 nm using different gas species in the pulsed jet and a variety of nozzle materials. All of the spectra presented here have not been corrected for the spectral response of the detection system. With lighter gases such as *He*, spectra dominated by emission from the gas species in the pulsed jet were obtained. An example of a spectrum obtained with *He* and a nozzle made of Macor is shown in Figure 5. All of the bright emission lines can be assigned to excited helium atoms and ions. To obtain this spectrum, the gate on the boxcar was set to a

width of 75 ns and was delayed 250 ns after the peak of the current pulse. This time window for observation was chosen because the spectra measured at various time delays indicated that many spectral lines were more prominent during this interval.

Using *Ar* and other heavier gases in the pulsed nozzle, however, the spectra obtained are quite different. While the visible spectrum obtained with *Ar* is dominated by lines from *Ar II* and *Ar III*, the VUV spectrum is dominated by lines from the sputtered nozzle material. Figure 6 shows the VUV spectrum obtained using *Ar* with a sapphire nozzle. The time interval for observation is identical to that used for the *He* spectrum. The dominant features are aluminum and oxygen lines originating from the sputtering of the sapphire (Al_2O_3) nozzle. Sputtering is due to the effective momentum transfer from the gas ions to the nozzle material. Typical ion kinetic energies inside the nozzle can be estimated to be 10 eV to several hundred eV. In this energy range efficient sputtering of the nozzle material by heavier rare gases is expected, whereas the sputtering efficiency of *He* is low[8].

To demonstrate that these spectral features are indeed almost independent of the gas medium, Figure 7 compares a spectrum obtained with *Kr* in the pulsed jet discharge and a spectrum obtained using *Ar*. Both spectra were obtained under identical conditions using the same nozzle with a 300 ns wide gate delayed 200 ns from the peak of the current pulse. The more intense spectrum using *Kr* was taken first, and then the *Ar* spectrum. The intensity of the spectral features which are due to emission from the nozzle material tends to weaken the longer the nozzle is used due to the widening of the orifice by the discharge. Also, the sputtering efficiency of *Kr* is higher than for *Ar* due to their mass difference. The striking similarity between both spectra and the fact that all prominent features can be assigned to emission from aluminum shows that consideration of the nozzle material is indeed crucial for the interpretation

of optical spectra from intense pulsed jet discharges.

When Macor is used as the nozzle material, the VUV spectra with the heavier gases are dominated with *Si* and *Al* lines. An example with *Ar* as the gas species is shown in Figure 8. The time interval for observation is again identical to that of the *He* spectrum in Figure 5. Macor has a complicated chemical composition, but some of the major constituents are SiO_2 (46%) and Al_2O_3 (16%). Spectra obtained with glass nozzles show many of the same *Si* lines. Spectra taken with carbon, PVC, or Delrin nozzles exhibit strong carbon lines.

The high degree of excitation and ionization apparent in all of the spectra is a result of the initial confinement of the discharge to the small orifice allowing very high current densities (~ 1 MA/cm^2) to be achieved. Some of the spectral lines which have been identified as arising from the sputtering of the nozzle material indicate the formation of states as much as 45 eV above the ground state of the neutral species. Such pulsed jet discharges could therefore have applications in spectroscopic studies of highly excited states of materials that are difficult to evaporate, or in the development of incoherent VUV light sources for other spectroscopic investigations.

In Ref. 1, emission from the excimer Ar_2^* around 126 nm was reported using a pulsed jet discharge with similar discharge parameters. In the work reported here, the region around 126 nm was extensively studied with various nozzles and at various discharge voltages, but no evidence of emission from Ar_2^* was detected. Searches for other excimer emissions - such as He_2^*, Kr_2^*, ArF, KrF, and XeF - were also performed, but no emission from these species in such a high current pulsed jet discharge was observed.

IV. Plasma Etching

Increased interest in micromechanics has created the need for faster etching mechanisms for a variety of materials. Recent work with continuous microwave discharges using a halogen containing gas has demonstrated a very high etching rate of silicon [9]. However, the limitations on the design of the nozzles for microwave discharges because of the need for impedence matching warrants exploration of other types of discharges which are more flexible in their design parameters to see if similar etch rates can be obtained. Chemical wet etching is either slow (typically about 1 μm/min) and/or has problems with masking, since the mask is also etched [10]. Dry etching processes are often slower (0.1 μm/min) and rarely exceed 10 μm/min [9]. The ability of the pulsed jet discharge to create highly ionized species motivated the study of its feasibility as a high etch rate mechanism when used in conjunction with a halogen containing gas.

Figure 9 shows the configuration used for etching. A stainless steel wire mesh was used as a test mask. The wire mesh was laid on top of the silicon wafer and mechanically held in place. The wafer was about 2 mm below the nozzle orifice. A discharge voltage of 10 KV was used as a compromise between etching speed and sharpness of the etching pattern. With lower voltages, the etching rate was slower, and at voltage of less than 8 KV, the discharge was not stable when using NF_3, as the gas species in the pulsed jet. At higher voltages, although the etch rate was somewhat larger, the etched pattern was less clear and some melting of the wire mesh occurred. The cleanest etching was observed using a sapphire nozzle, since this material was the most resistant against sputtering.

Scanning electron micrographs of an etched sample are shown in Figure 10. The distance between the wires of the mesh was about 35 μm in this case. Optical microscopy indicated that

the etched features were about 50 μm deep at the deepest point. Although further optimization of the discharge parameters will be necessary to obtain sharper features, it is encouraging that by optimizing only two parameters, the discharge voltage and the distance between the nozzle and the wafer, the wire mesh pattern could be replicated in the etched wafer.

Both NF_3 and SF_6 were used as the gas species for etching. Better results were obtained with NF_3, possibly because the electron temperature is high enough that the dissociative attachment coefficient of NF_3 to form F^- exceeds that of SF_6 [11]. If Ar instead of a halogen containing gas was used in the pulsed jet discharge, there was no observable etching; therefore, the etching is primarily chemical and not mechanical or thermal. The system was operated at 50 Hz, limited only by problems of heat dissipation in the nozzle. Figure 11 shows the average of the deepest etch depth of several experiments as a function of the time with the discharge system operating at 50 Hz with a voltage of 10 KV. A least squares fit indicates an etch rate of approximately 12 μm/min. With further improvements to the construction of the nozzles, so that the heat dissipation can be increased, it is anticipated the repetition rate of the discharge could be increased to further improve the etch rate to approximately 100 μm/min as reported in Ref. [9].

V. Conclusion

The characterization of a pulsed jet discharge has been performed and possible applications to VUV spectroscopy and micromechanics were explored.

The applications to VUV spectroscopy include the study of very highly excited states of atoms and ions of low vapor pressure materials such as Al and Si. These species are produced by the sputtering of the nozzle material in the high energy region of the nozzle orifice when heavy gases such as Ar or Kr are used.

The feasibility of using a pulsed jet discharge in conjunction with a halogen containing gas as a high etch rate mechanism for silicon has also been demonstrated. Etch rates of about 12 μm/min have been achieved using NF_3.

VI. Acknowledgment

We would like to thank Drs. B. Stoicheff, G. Eden, and K. Midorikawa for helpful discussions and for sharing their related work with us. This research was supported by the National Science Foundation, the Air Force Office of Sponsored Research, the Office of Naval Research, and the Robert A. Welch Foundation.

References:

[1] T. Epthimiopoulos, B.P. Stoicheff, and R.I. Thompson, "Efficient Population Inversion in Excimer States by Supersonic Expansion of Discharge Plasmas," *Opt. Lett.* 14, 624-626 (1989).

[2] C. Jouvet, C. Lardeaux-Dedonder, and D. Solgadi, "Fluorescence Excitation Spectra of the *XeCl(B,C)* States in a Supersonic Jet," *Chem. Phys. Let.* 156 (6), 569-572 (21 April 1989).

[3] C.S. Feigerie and J.C. Miller, "Multiphoton Ionization of Vibrationally Hot Nitric Oxide Produced in a Pulsed Supersonic Glow Discharge," *J. Chem. Phys.* 90 (6), 2900-2908 (15 March 1989).

[4] K.G.H. Baldwin, R.P. Swift, and R.O. Watts, "Inert Gas Excimer Radiation from a Free Jet Expansion," *Rev. Sci. Instrum.* 58 (5), 812-816 (May 1987).

[5] P.C. Engelking, "Corona Excited Supersonic Expansion," *Rev. Sci. Instrum.* 57 (9), 2274-2277 (September 1986).

[6] K.P. Huber and T.J. Sears, "Emission Spectra in a Supersonic Expansion: The Quartet System of *NO* and the Schüler Band of ND_4," *Chem. Phys. Let.* 113 (2), 129-134 (11 January 1985).

[7] A.T. Droege and P.C. Engelking, "Supersonic Expansion Cooling of Electronically Excited Radicals," *Chem. Phys. Let.* 96 (3), 316-318 (8 April 1983).

[8] A.B. Glaser, G.E. Subak-Sharpe, Integrated Circuit Engineering, Reading, MA, Addison-Wesley, 1977,pp. 169-181.

[9] L. Bárdos, S. Berg, and H.O. Blom, "Superhigh-rate Plasma Jet Etching of Silicon," *Appl. Phys. Lett.* 55 (16), 1615-1617 (16 October 1989).

[10] K.E. Petersen, "Silicon as a Mechanical Material," *Proceedings of the IEEE* 70 (5), 420-457 (May 1982).

[11] P.J. Chantry, "Negative Ion Formation in Gas Lasers," *Applied Atomic Collision Physics* 3, ed. by E.W. McDaniel and W.L. Nighan, New York; Academic Press, 1982, pp. 35-70.

Figure Captions:

Figure 1: Schematic of the pulsed jet discharge and the VUV detection apparatus.

Figure 2: Schematic of the high voltage circuit.

Figure 3: Discharge voltage and current waveforms.

Figure 4: Traces of the temporal behavior of the intensity of the 207 nm emission of *Si II* at *(a)* 15 KV and *(b)* 20 KV.

Figure 5: Emission spectrum at 15 KV charging voltage, taken 250 ns after the peak of the current pulse, with *He* as the gas species and using a Macor nozzle.

Figure 6: Emission spectrum at 17.5 KV charging voltage, taken 250 ns after the peak of the current pulse, with *Ar* as the gas species and using a sapphire nozzle.

Figure 7: Comparison of the emission spectra using a sapphire nozzle with *Kr* and *Ar* as the gas species. Both spectra were taken under identical conditions with the gate delayed 200 ns after the peak of the current pulse.

Figure 8: Emission spectrum at 15 KV charging voltage, taken 250 ns after the peak of the current pulse, with *Ar* as the gas species and using a Macor nozzle.

Figure 9: Schematic of the pulsed jet discharge when used for plasma etching.

Figure 10: Scanning electron micrographs of an etched silicon wafer. *(a)* View of the entire etched area, approximately 1/8" in diameter. *(b)* Detail of same wafer. The distance between the wires was approximately 35 μm. The depth at the deepest etch point was about 50 μm.

Figure 11: Average over several runs of the deepest etch depth in a silicon wafer vs. the time the system was operated at 50 Hz. NF_3 was used as the gas, and the discharge was operated at 10 KV.

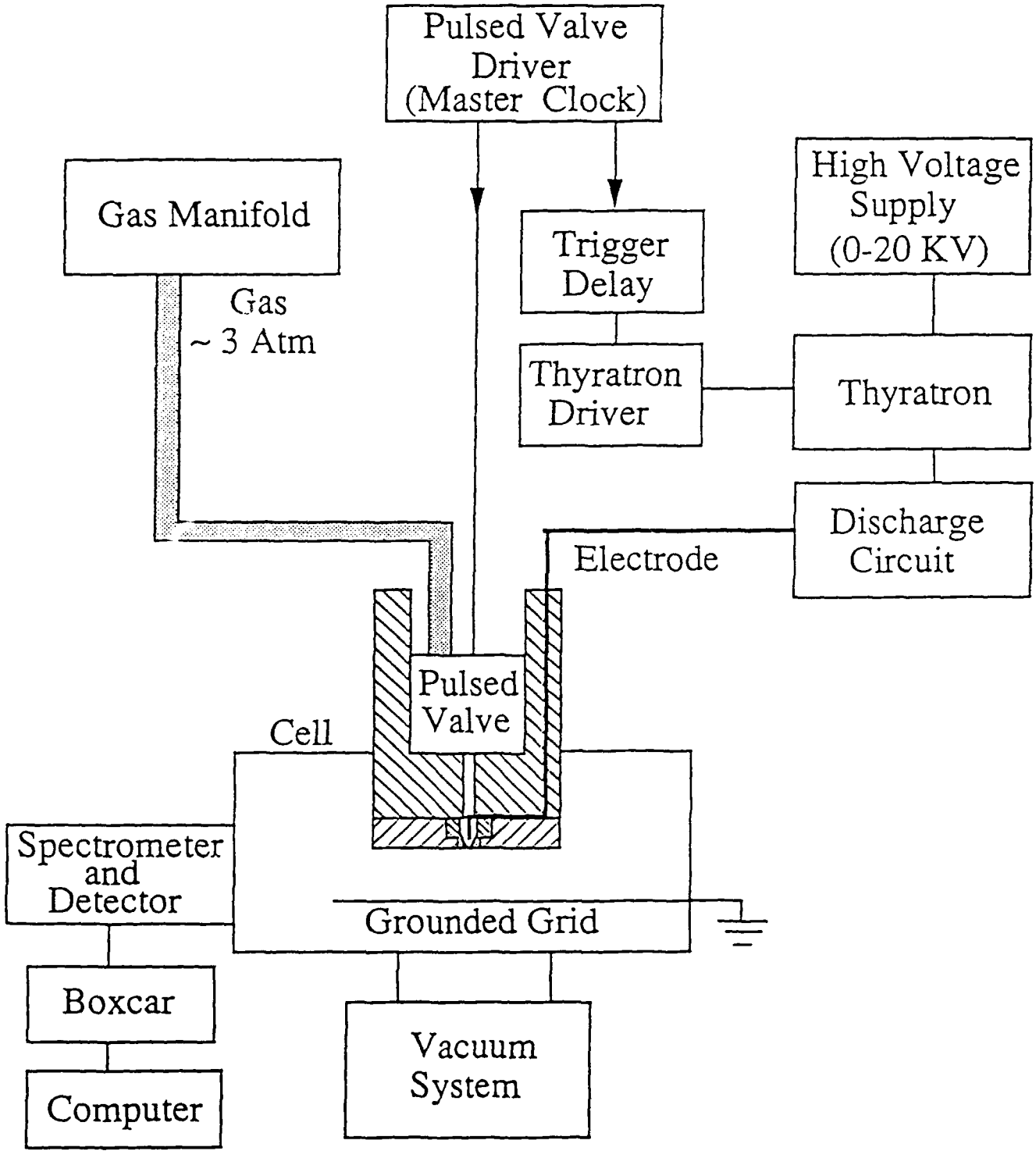
Pulsed Valve Driver (Master Clock)
Gas Manifold
Gas ~ 3 Atm
Trigger Delay
High Voltage Supply (0-20 KV)
Thyratron Driver
Thyratron
Discharge Circuit
Electrode
Pulsed Valve
Cell
Spectrometer and Detector
Grounded Grid
Boxcar
Computer
Vacuum System

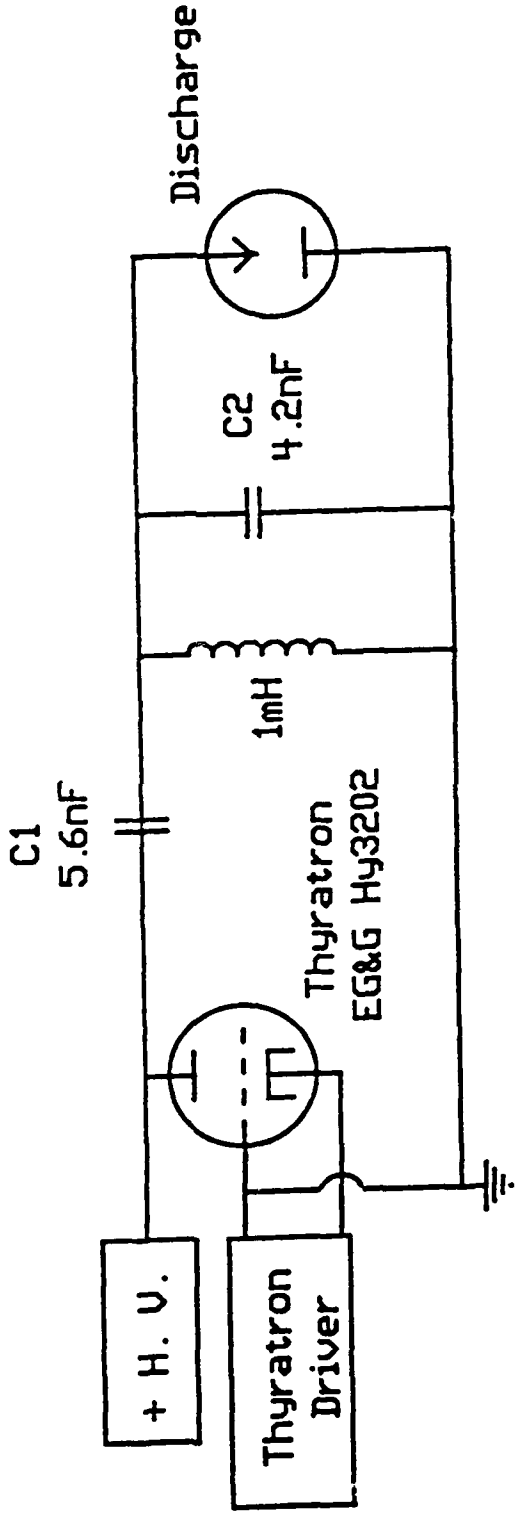
Discharge
C2
4.2nF
1mH
C1
5.6nF
Thyratron
EG&G Hy3202
+ H. V.
Thyratron
Driver

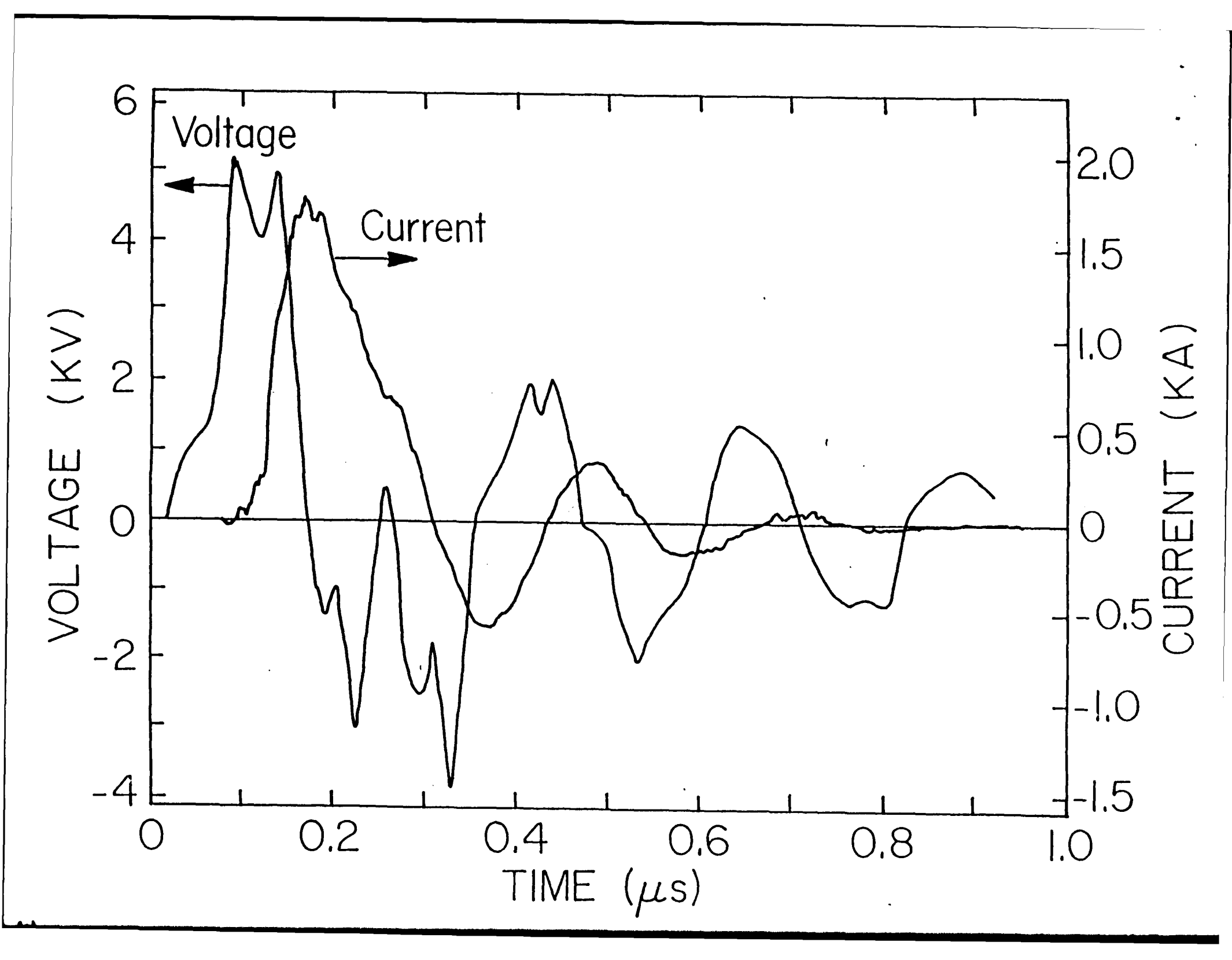
Voltage
Current
VOLTAGE (KV)
CURRENT (KA)
TIME (μs)
6
4
2
0
-2
-4
2.0
1.5
1.0
0.5
0
-0.5
-1.0
-1.5
0
0.2
0.4
0.6
0.8
1.0

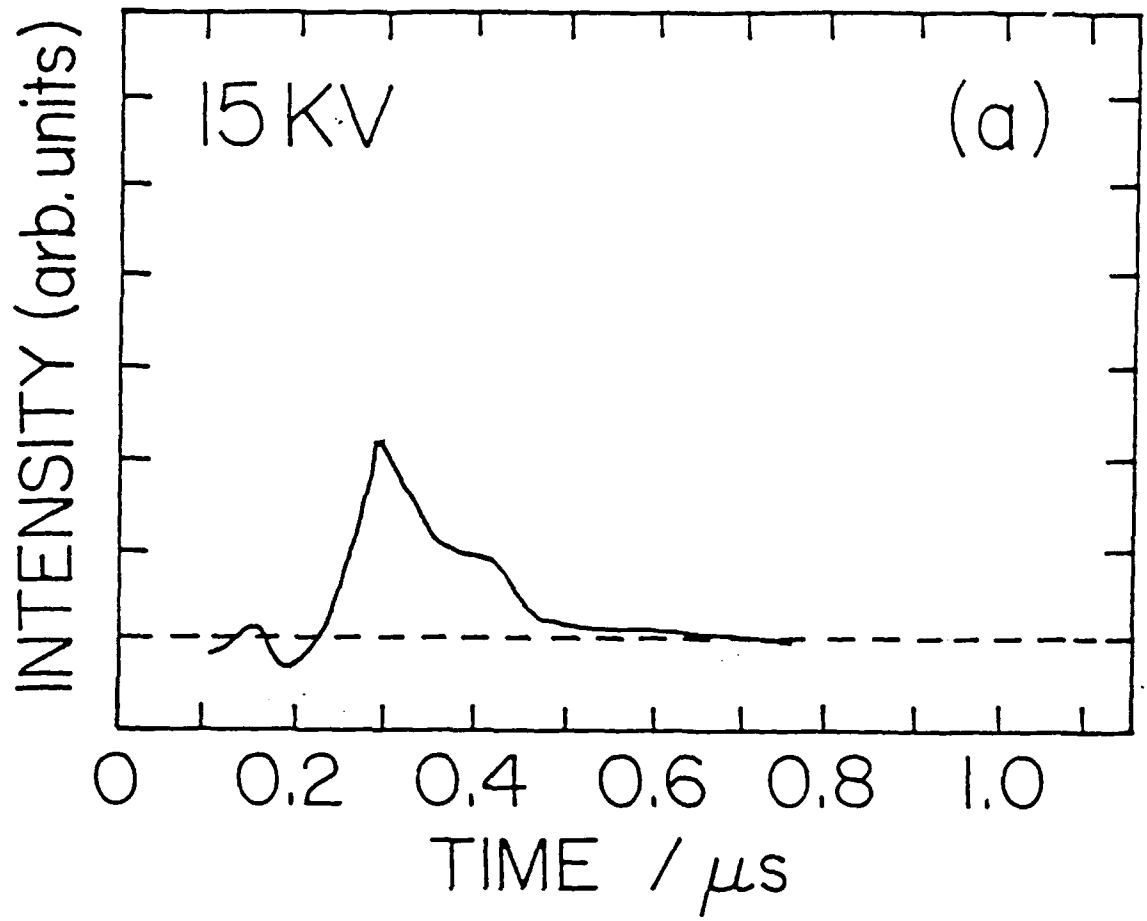
15 KV
(a)
INTENSITY (arb. units)
0
0.2
0.4
0.6
0.8
1.0
TIME / μs

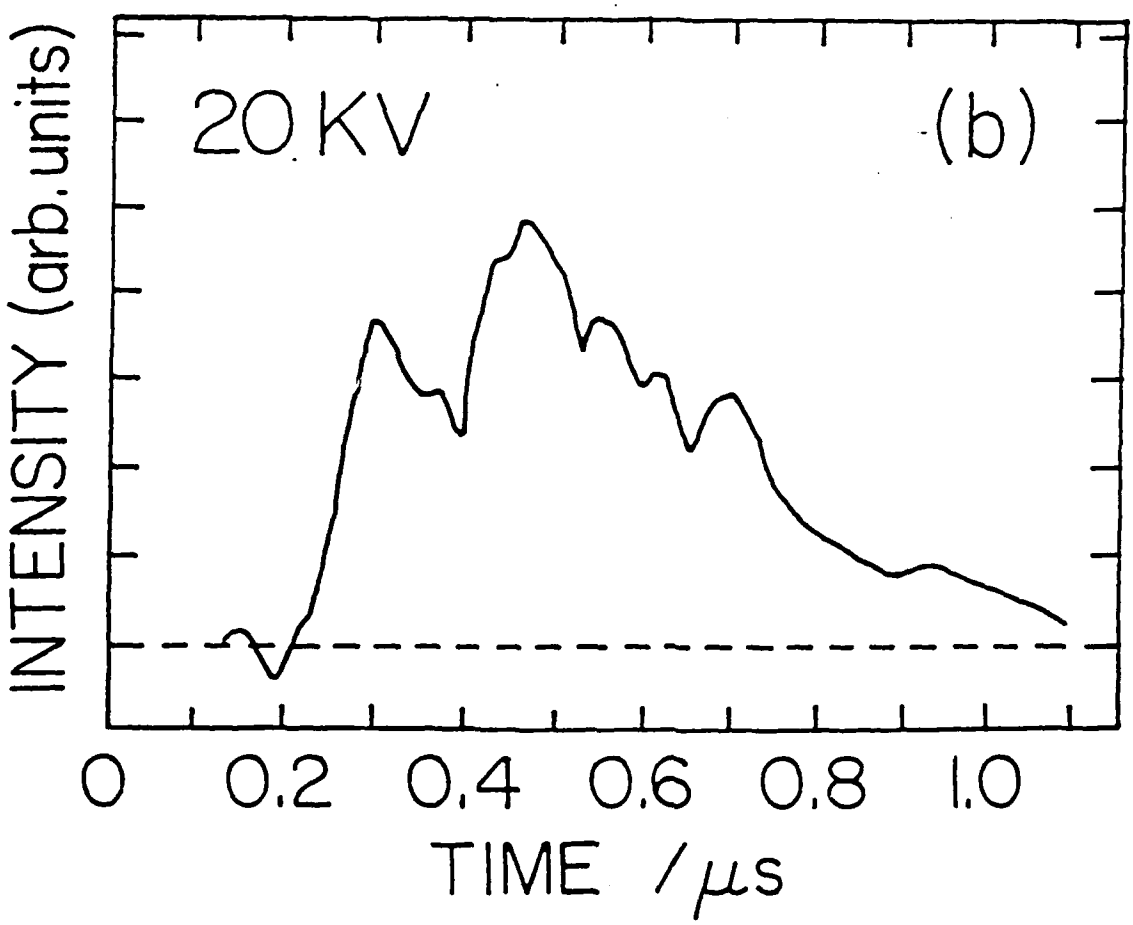
20 KV
(b)
INTENSITY (arb. units)
0
0.2
0.4
0.6
0.8
1.0
TIME / μs

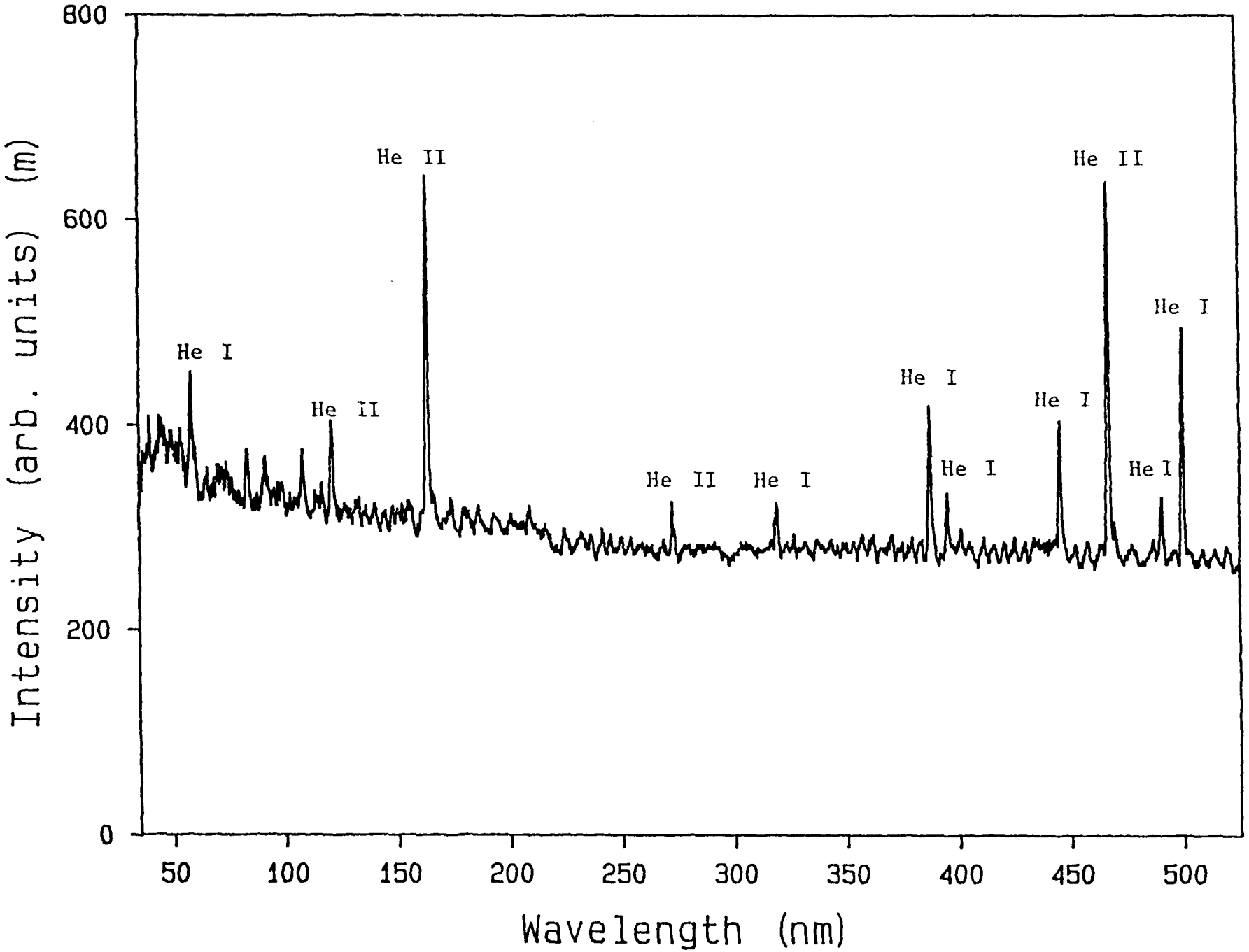
800
600
400
200
0
Intensity (arb. units) (m)
He I
He II
He II
He II
He I
He I
He I
He I
He II
He I
He I
50
100
150
200
250
300
350
400
450
500
Wavelength (nm)

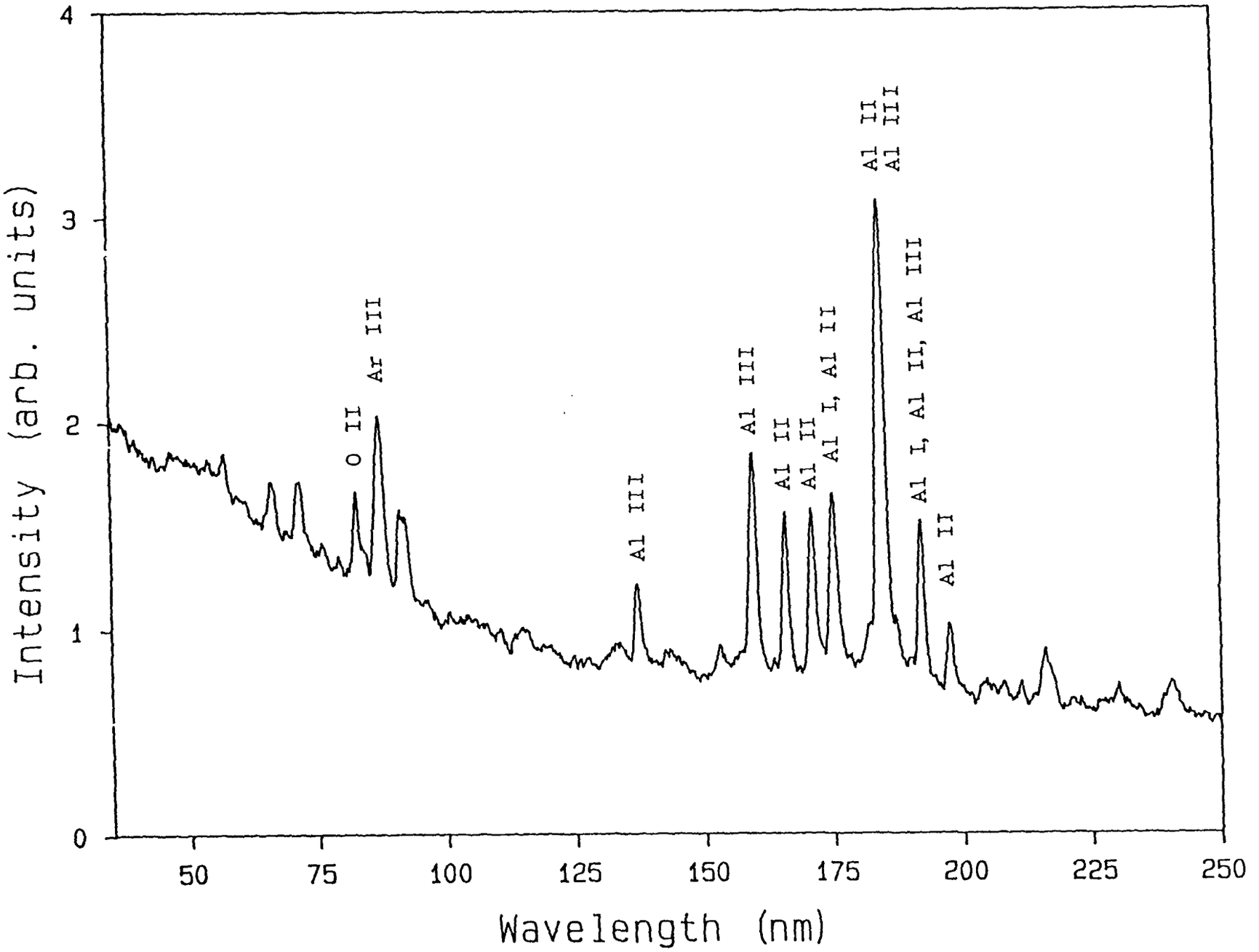
Intensity (arb. units)
Wavelength (nm)
0
1
2
3
4
50
75
100
125
150
175
200
225
250
O II
Ar III
Al III
Al III
Al II
Al II
Al I, Al II
Al II
Al II
Al I, Al II, Al III
Al I, Al II, Al III

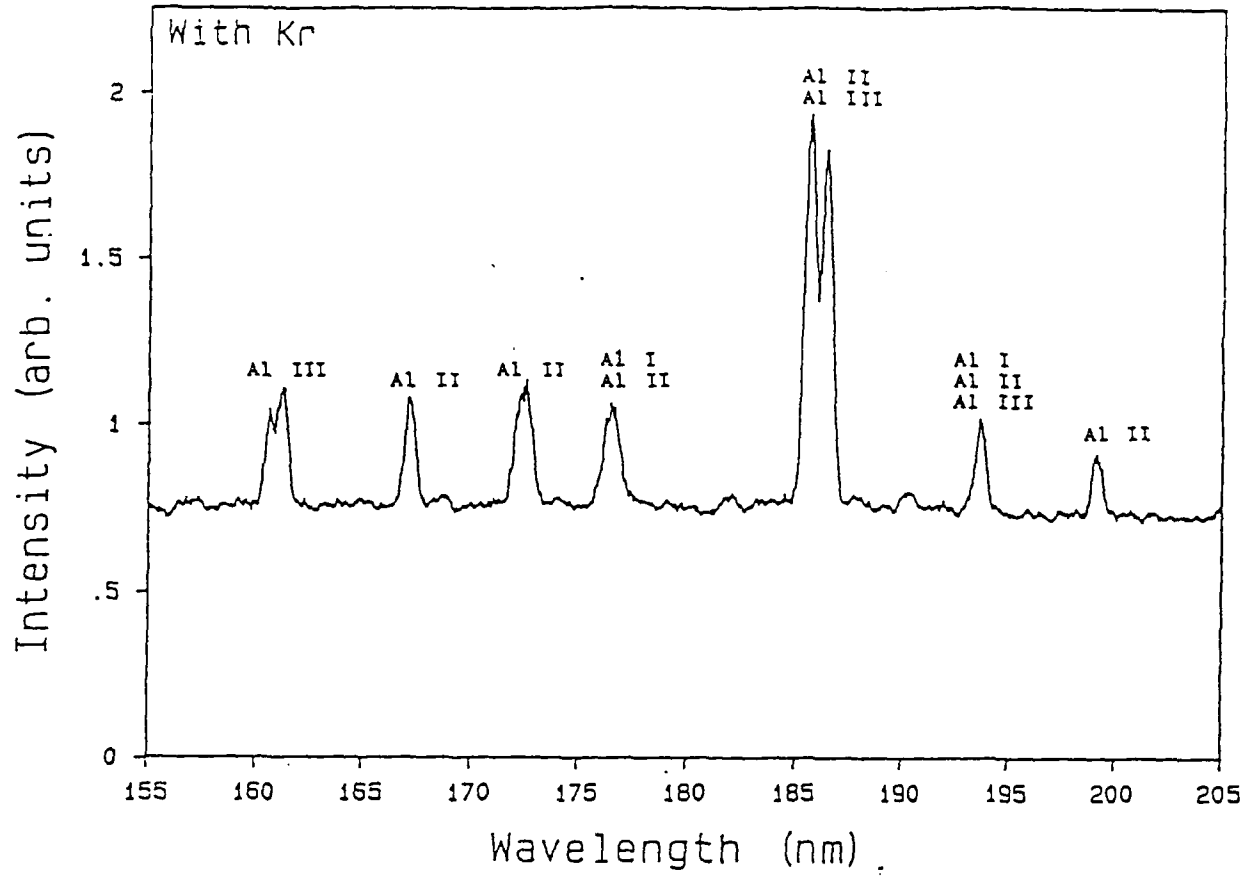
With Kr
Intensity (arb. units)
Wavelength (nm)
Al III
Al II
Al II
Al I
Al II
Al II
Al III
Al I
Al II
Al III
Al II
0
.5
1
1.5
2
155
160
165
170
175
180
185
190
195
200
205

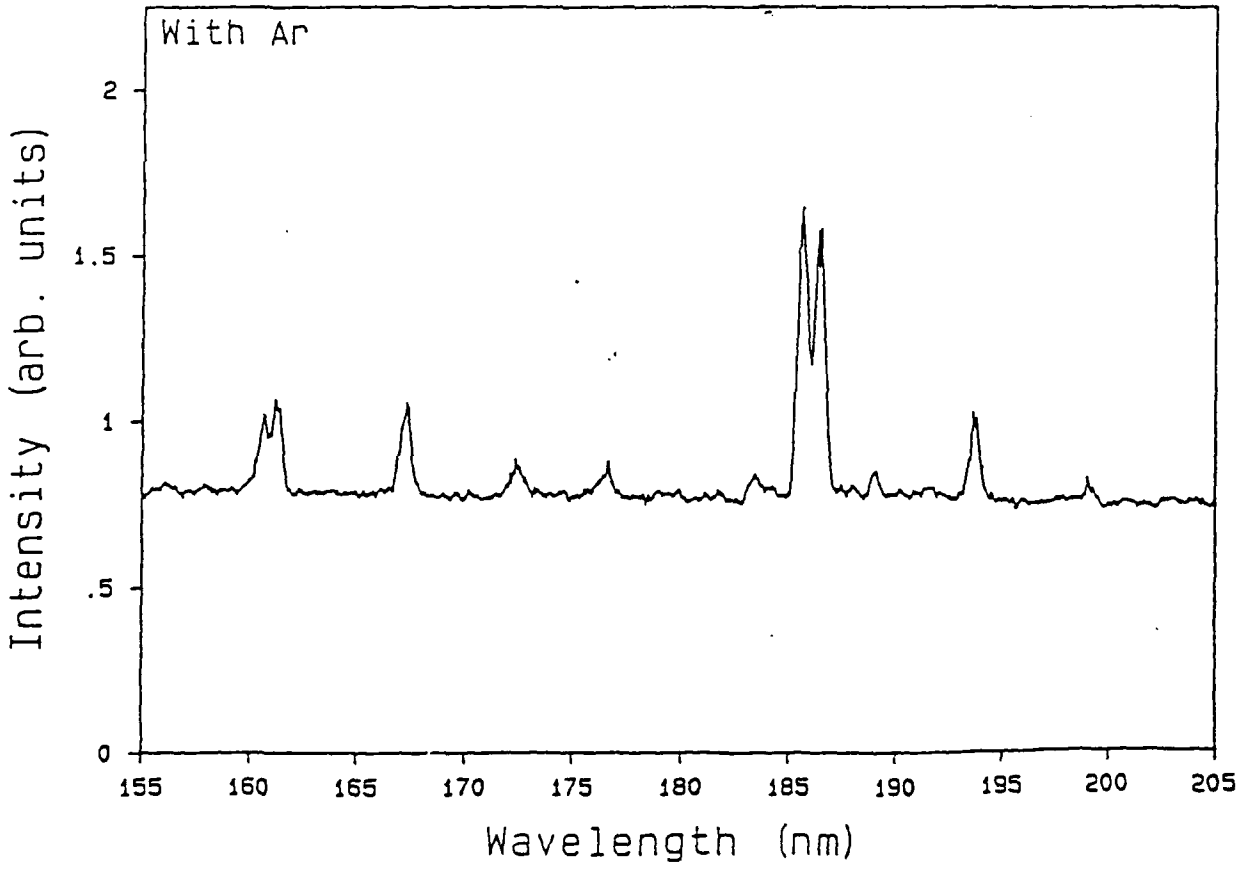
With Ar
Intensity (arb. units)
Wavelength (nm)
0
.5
1
1.5
2
155
160
165
170
175
180
185
190
195
200
205

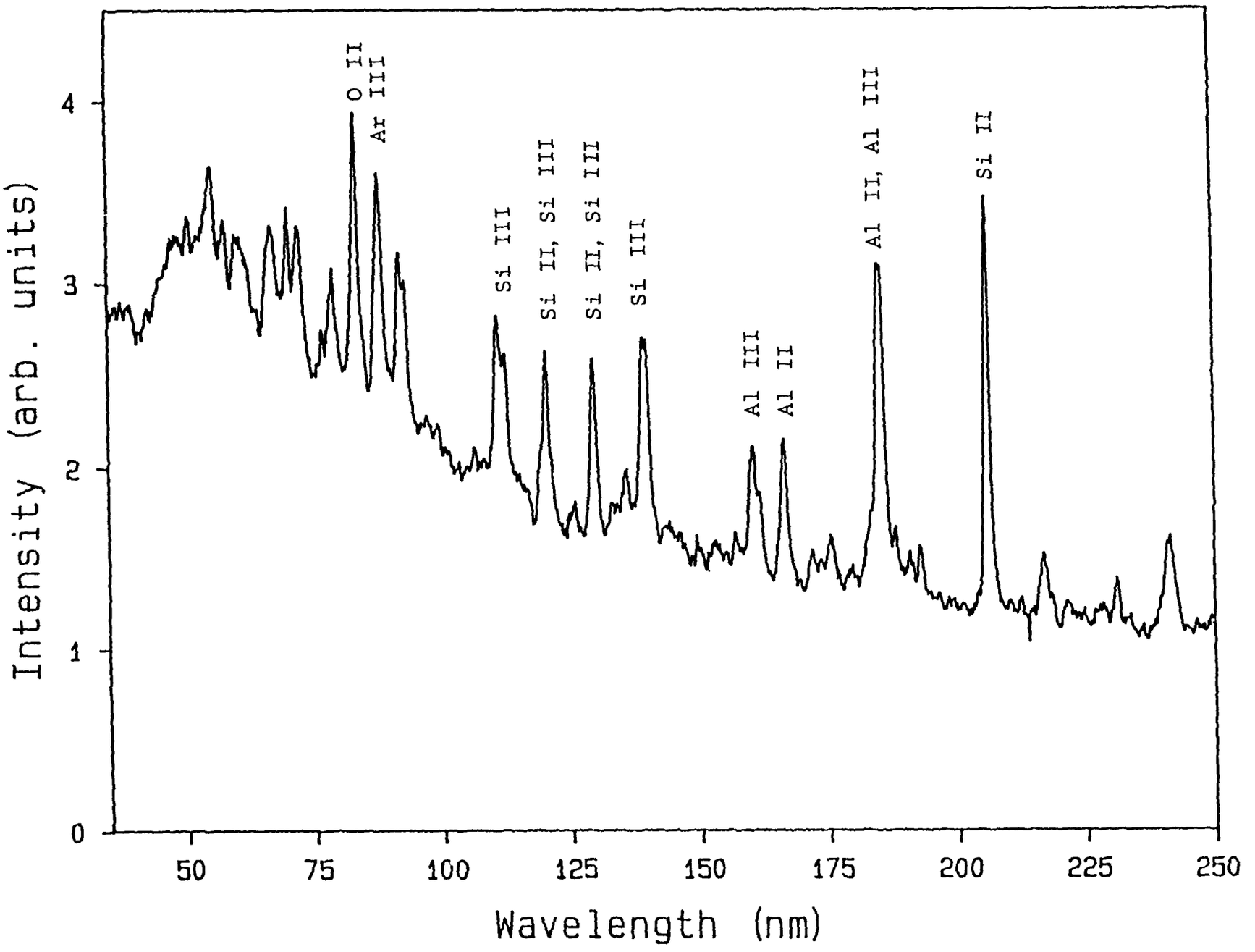
O II
Ar III
Si III
Si II, Si III
Si II, Si III
Si III
Al III
Al II
Al II, Al III
Si II
Intensity (arb. units)
0
1
2
3
4
50
75
100
125
150
175
200
225
250
Wavelength (nm)

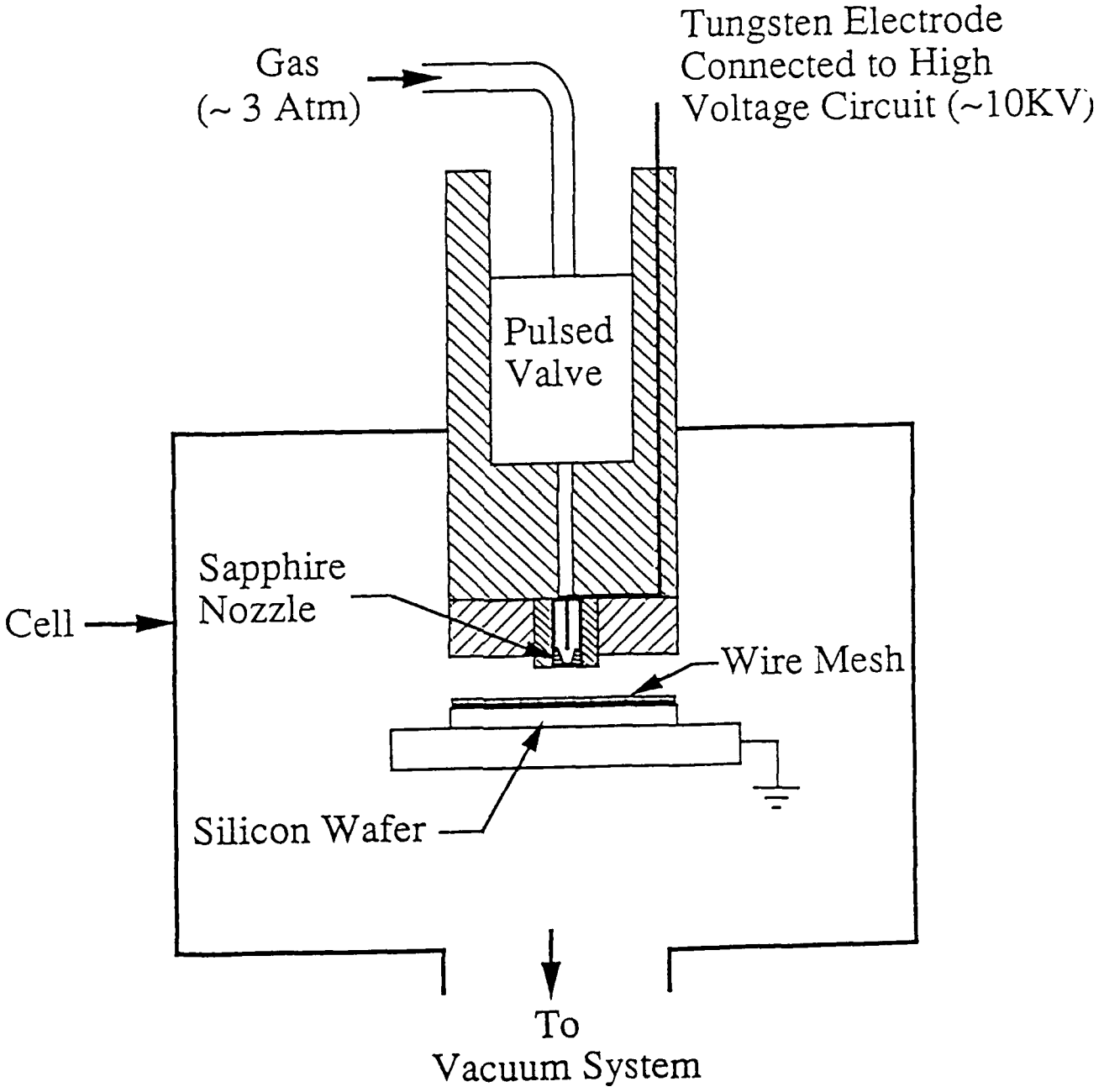
Gas
(~ 3 Atm)
Tungsten Electrode
Connected to High
Voltage Circuit (~10KV)
Pulsed
Valve
Sapphire
Nozzle
Cell
Wire Mesh
Silicon Wafer
To
Vacuum System

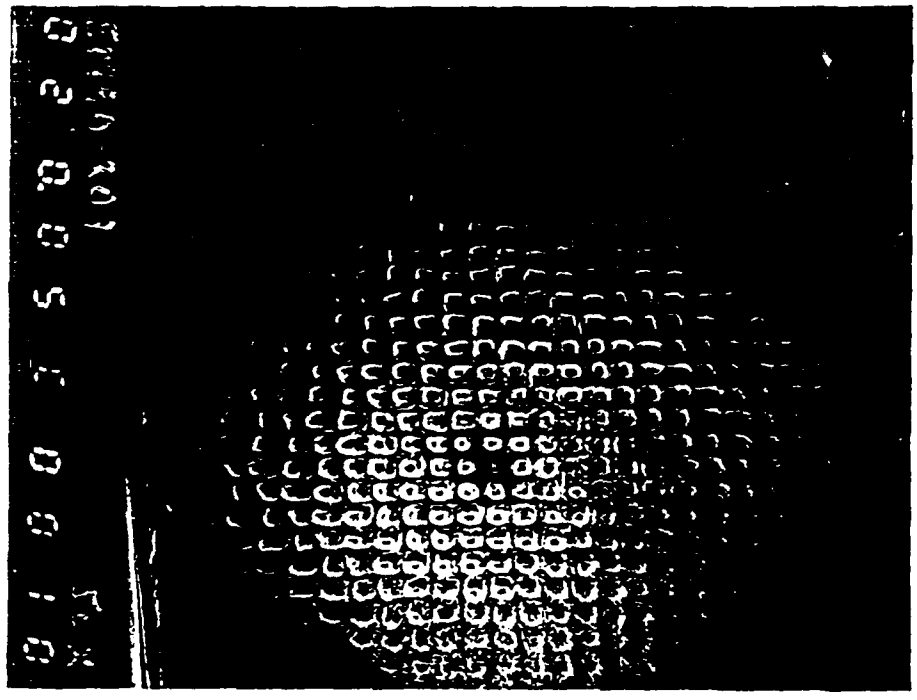

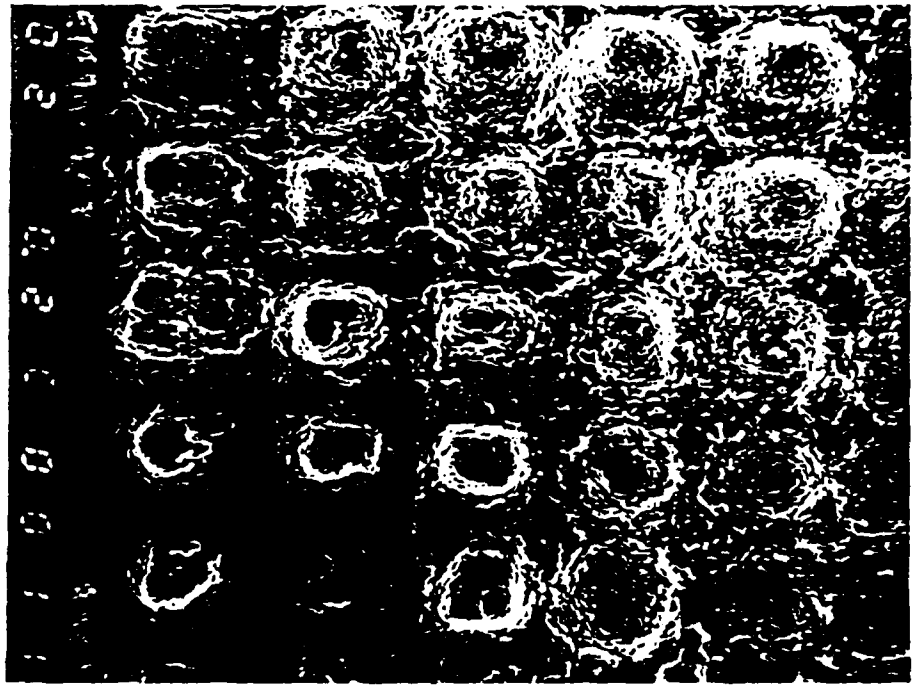

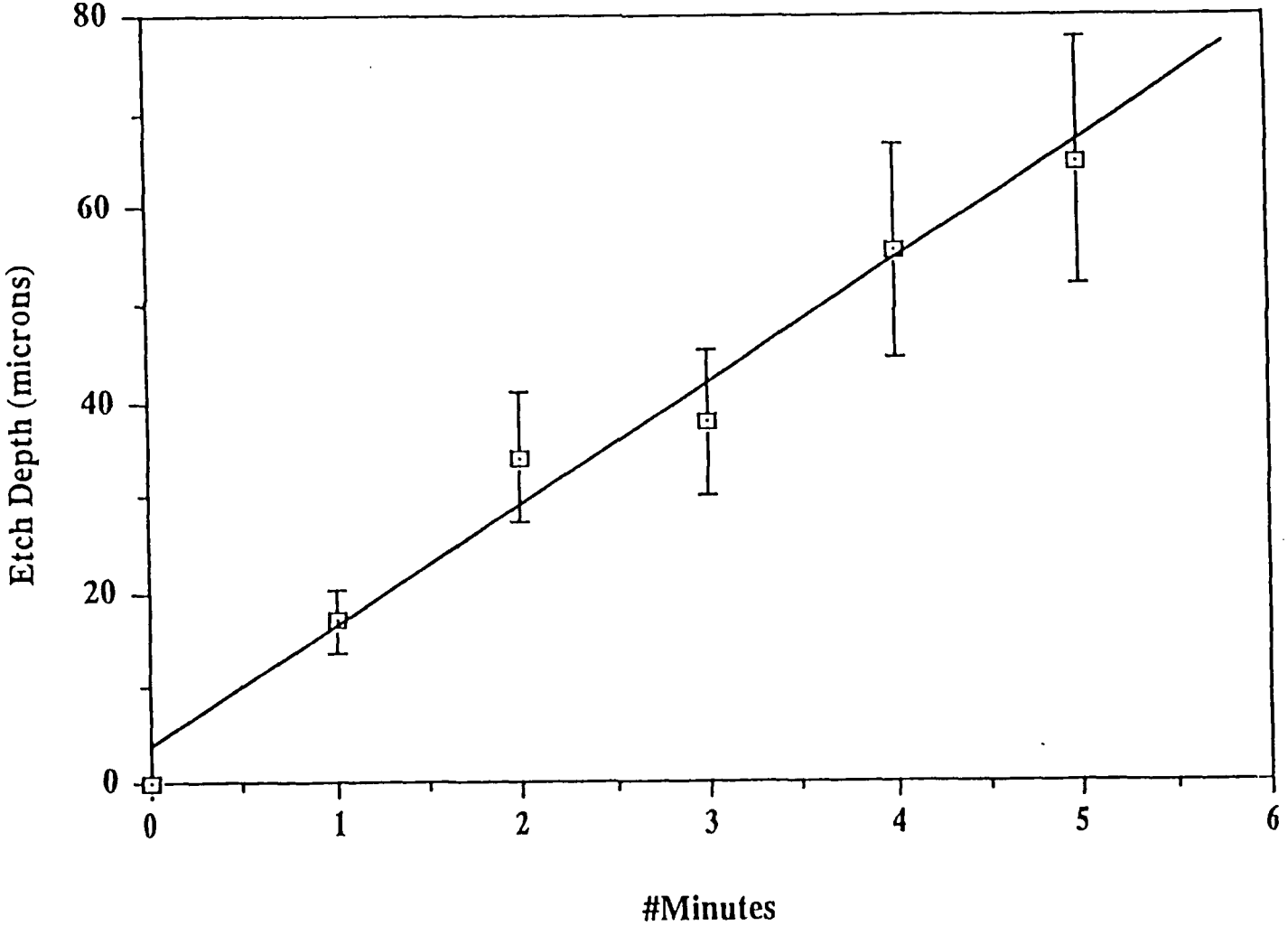
80
60
40
20
0
Etch Depth (microns)
0
1
2
3
4
5
6
#Minutes